Radiation-Conduction interaction of steady streamwise surface temperature variations on vertical free convection.

A Dissertation Submitted in Partial fulfillment of the
requirements for the award of the degree

of
Master of Philosophy
in Mathematics

By
MD. KUTUB UDDIN
Registration no. 9509003, Session 1994-95-96
Department of Mathematics
Bangladesh University of Engineering and Technology
Dhaka-1000

Supervised & approved

By

Dr. Md. Mustafa Kamal Chowdhury
Department of Mathematics

Bangladesh University of Engineering and
Technology, Dhaka-1000

The Thesis Entitled
Radiation-Conduction interaction of steady streamwise surface temperature variations on vertical free convection.
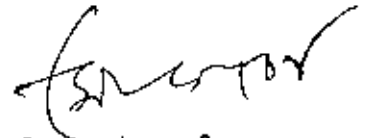
Submitted By

MD. KUTUB UDDIN
Registration no 9509003, Session 1994-95-96, a part time student of M. Phil (Mathematics) has been accepted as satisfactory in partial fulfillment for the Degree of
Master of Philosophy in Mathematics
on 12th April, 2001.

Board of Examiners

1. **Dr. Md. Mustafa Kamal Chowdhury**
   Professor
   Department of Mathematics,
   BUET, Dhaka-1000

   Supervisor &
   Chairman

2. **Head**
   Department of Mathematics
   BUET, Dhaka-1000

   Member

3. **Md. Abdul Quddus Mean**
   Associate Professor
   Department of Mathematics
   BUET, Dhaka-1000

   Member

4. **Dr. A. K. M. Sadrul Islam**
   Professor
   Department of Mechanical Engineering
   BUET, Dhaka-1000

   Member
   (External)

CANDIDATE'S DECLARATION

I here by certify that the work which is being presented in the thesis entitled "Radiation-Conduction interection of steady streamwise surface temperature variations on vertical free convection", a dissertation submitted in partial fulfillment of the requirements for the award of the degree of Master of Philosophy in Mathematics, submitted in the Department of Mathematics of Bangladesh University of Engineering and Technology, Dhaka, is an authentic record of my own work.

The matter presented in this thesis has not been submitted by me for the award of any other degree of this or any other University.

Md. Kutub Uddin

Acknowledgement

Abstract

We examine how the steady free convective boundary-layer flow induced by a vertical heated surface is affected by the presence of sinusoidal surface temperature variations about a constant mean value with the effect of radiation. Besides this, we have also analyze the effect of radiation of staady streamwise surface temperature variation of a vertical cone. The problem is studied using fully numerical techniques. The surface rate of heat transfer eventually alternates in sign with distance from the leading edge, but no separation occurs unless the amplitude of the thermal modulation is sufficiently high. Numerical results are obtained for different values of the physical parameters, the radiation parameter R_d, Prandtl number Pr and the surface temperature wave amplitude a.

Important aspects of the overall behavior of our analysis by observing that the boundary layer is thinner when the surface temperature is relatively high and thicker when it is low. This arises because relatively high surface temperatures induce relatively large upward fluid velocities with the consequent increase in the rate of entrainment into the boundary layer. This causes, in turn, a thinning of the boundary layer. Thus, we should expect high shear stresses and rates of heat transfer at, or perhaps just beyond, where the surface temperature attains its maximum values. As x increases, the amplitude of oscillation of the rate of heat transfer curves increases gradually, and the amplitude of oscillation of the shear stress curve decreases slowly, with x.

The most interesting part of this analysis is that, when radiation parameter R_d is increasing, both the shear stress and the rate of heat transfer are also increasing but when $R_d = 0$. the result of rate of heat transfer is exactly the same, which was found by Rees [14]. In our study we have found that rate of

heat transfer is increasing as R_d is increasing but at a decreasing rate. That is, when $R_d = 1$ then rate of heat transfer increased more in respect of R_d =10.

Nomenclature

a	Surface temperature wave amplitude
a_R	Rosseland mean absorption coefficient
f	Dimensionless velocity function
g	Dimensionless temperature
Gr	Grashof number
Pr	Prandtl number
d	Half the dimensional thermal wave length
R_d	Radiation Parameter
p	Pressure
u, v	Velocity components
T	Temperature of the fluid
T_α	Temperature of the ambient fluid
x, y	Streamwise and cross stream Cartesian coordinate
ψ	Stream function
σ	Stefan-Boltzman constant
σ_s	Scattering coefficient
β	Coefficient expansion
ν	Kinematic coefficient of viscosity
η	Psuedo-similarity variable
ξ	Dimensionless x coordinates
θ	Temperature
θ_w	Surface Temperature parameter
ρ	Density of the fluid
T_w	Mean-surface temperature to the wall
q_r	radiative flux
κ_λ	absorption coefficient
$e_{b\lambda}$	Planck function

Table of Contents

Chapter 1

Introduction

Man's study of the Universe has led to the realization that all physical phenomena are subject to natural laws. The term nature might well be used to describe the framework or system. Of fundamental and universal importance within this system are the mechanisms for the transfer of energy. The mention of mechanisms suggests the familiar process of conduction convection and radiation. These so called modes of heat transfer are standard and widely used concepts, not only in engineering but also in all fields of natural science. They have been adopted by the engineer from the natural scientist.

The formation of a physical picture of the process of thermal conduction is a simple task for the imagination. It is a matter of experience that heat flows from a region of higher to one at a lower temperature. Since temperature is considered an index of degree of molecular activity, it is logical to picture energy transfer as occurring by collision of faster with slower moving molecules. This idea appears to essentially correct. In the case of gasses, molecular interaction is responsible; however, in solids such as metals an 'electron gas' –rather than molecules –is the primary energy transfer medium.

The mechanism of convection is simply the transfer of energy by actual physical movement from one location to another of a substance in which energy is stored. The free or forced movement of hot air throughout a room to provide is a familiar example. The process may not seem quite so elementary when we begin to deal with heat transfer in complex fluid flows. But this as it may, to understand the principle of convection one need only visualize the displacement of usually small quantities of matter inescapably carrying along their various forms of stored energy.

1

Energy transfer by radiation is usually considered last, probably because radiation is more of a mystery. It is very difficult to provide a simple mental or physical picture of something, which is quite invisible and travels with infinite ease through empty space. Its manifestations have been extensively studied, however, and we are able to deal with it at least in the spirit expressed by Oliver Heaviside when he said, "Shall I refuse my dinner because I do not understand the process of digestion?"

Whether radiation is a wave or corpuscular phenomenon has long been subject to controversy. The establishment of the electromagnetic theory in the latter half of the nineteenth century seemed to be a victory for the wave hypothesis, but the introduction and subsequent success of the quantum theory have indicated corpuscular nature.

It is possible that in the final analysis we may not find the various modes of heat transfer to be fundamentally different. The true nature of energy is of such a subtle character that it is still beyond our understanding and description. More insight into its basic qualities could well prove that unrelated phenomena are different manifestations of the same fundamental process This is already becoming evident in connection with radiation and conduction. The quantum theory has been equally useful in explaining thermal phenomena in solids as well as radiation effects.

In dealing with heat transfer from an engineering point of view, we might overlook such matters since only macroscopic effects are considered. Although this is, in general, permissible, we must remember our objective, which is the continued application of basic knowledge for the advancement of humanity. This we can accomplish only by regular review of fundamental progress, alertness in its use in the interpretation of our work, and its possible applications.

The study of heat transfer is of great interest in many branches of science and engineering. In the design of heat exchangers such as boilers, condensers, radiators, etc., for example, heat transfer analysis is essential for sizing such

equipment. In the design of nuclear-reactor cores, a thorough heat transfer analysis of fuel elements is important for proper sizing of fuel elements to prevent burnout. In aerospace technology, heat transfer problems are crucial because of weight limitations and safety considerations. In heating and air conditioning applications for buildings, a proper heat transfer analysis is necessary to estimate the amount of insulation needed to prevent excessive heat loses or gains.

The three distinct modes of heat transfer, namely conduction, convection and radiation must be considered. In reality, the combined effects of these three modes of heat transfer control temperature distribution in a medium. Conduction occurs if energy exchange takes place from the region of high temperature to that of low temperature by the kinetic motion or direct impact of molecules, as in the case of fluid at rest, and by the drift of electrons, as in the case of metals. The radiation energy emitted by a body is transmitted in the space in the form of electromagnetic waves. Energy is emitted from a material due to its temperature level, being larger for a larger temperature, and is then transmitted to another surface, which may be vacuum or a medium, which may absorb, reflect or transmit the radiation depending on the nature and extend of the medium. Considerable effort has been directed at the radiative mode of heat transfer. In this mode, relative motion of the fluid provides an additional mechanism for energy transfer. A study of radiative heat transfer involves the mechanisms of conduction and, sometimes, those of radiation processes as well. This makes the study of radiative mode a very complicated one.

In many cases of practical interest forced and natural convection processes are important. Heat transfer by mixed convection is one in which neither forced convection nor natural convection is predominant. A heated body lying in still air loses energy by natural convection. But the body generates a buoyant flow above it. If another body is placed in that flow, the body is subjected to an external flow. Now it becomes essential to determine the natural as well as the forced convection effects and the region in which the heat transfer occurs.

3

Though natural convection process is much more complicated than that of forced convection, yet the study of natural convection process is also important because of the problem of heat rejection and removal in many devices, processes and systems. Natural convection represents a limit on the heat transfer rates and this becomes a very important consideration for problems in which other modes are either not possible or not practical. It is also relevant for safety consideration under conditions when the usual mode fails and the system has to depend on natural convection to get rid of the generated heat. To overheating such consideration in design are essential in many electronic devices and system and in power generation.

Free convection flow and heat transfer problems is an important consideration in the thermal design of a variety of industrial equipment and also in nuclear reactors, geophysical fluid dynamics. The problem of boundary layer with transpiration has become very important in recent times; in particular in the field of aeronautical engineering; in actual applications it is often necessary to prevent separation in order to reduce drag and to attain high lift.

We have described an investigation of the combined effects of surface temperature variations and radiation on the steady boundary-layer flow of a Newtonian fluid from a heated vertical surface. It is well known that power-law surface temperature distributions (and also power-law surface heat fluxes) give rise to self-similar boundary layer flows [26, 16]. But here we are interested in another form of surface variation, namely, sinusoidal variations about a mean temperature, which is held above the ambient temperature of the fluid. As in [14] this type of surface distribution may be taken as a simplified model of the effects of a periodical array of heaters behind or within the heated surface. An accurate analysis of such a configuration requires a detailed examination of the effects of solid conduction within the heated surface, but the aim of the present work is to simplify the problem by imposing a surface temperature distribution. In this way we can determine a large amount of information about the resulting flow using both numerical methods.

Various papers have been published which deal with the effects of surface variations. For example. Yao [25] and Moulic and Yao [30, 31] have sought to investigate the effects of streamwise surface undulations of free and mixed convection from vertical surfaces held at uniform temperatures. More recently, Chiu and Chou [3], Hossain et. al. [22] and Kim [15] have extended these analyses to micropolar fluids, magnetohydrodynamic convection and non-Newtonian convection, respectively. In a series of papers Rees and Pop [8-12] and Rees [13] have also considered a large variety of analogous flows in porous media. Of these, only [14] has been concerned with the effect of sinusoidal surface temperature variations, although in that case the surface variations were spanwise, thereby giving rise to a three-dimensional flow-field.

A significant numbers of authors have investigated laminar free convection for two-dimensional axisymmetric flows. Mark and Prins [34-35] developed the general relations for similar solutions on isothermal axisymmetric forms and showed that the vertical cone has such a solution. Approximate boundary layer techniques were utilized to arrive at an expression for the dimensionless heat transfer. Broun et al. [36] contributed two more isothermal axisymmetric bodies for which similar solutions exist, and used an integral method to provide heat transfer results for these and the cone over a wide range of Prandtl number. Similarity solutions for free convection from the vertical cone have been exhausted by Hering and Grosh [37]. They showed that the similarity solutions to the boundary layer equations for a cone exist when the wall temperature distribution is a power function of distance along a cone ray. In their investigation, they presented the results by numerical integration of the transformed equations for non-isothermal temperature distributions for Prandtl number equals to 0.7. Latter, Hering [38] extended the enalysis to investigate for low Prandtl numbers. The study of Hering and Grosh [37] has also been extended by Roy [39] to treat the case of high Prandtl number fluid.

Effect of slenderness on the natural convection flow over a slender cone with constant wall heat flux has been studied by Na and Chiou [40]. The problem of natural convection flow over a frustum of a cone without transverse curvature effect

(i.e., large cone angles when the boundary layer thickness is small compared with the local radius of the cone) has been treated in the literature, even through the problem for a full cone has been treated quite extensively by Sparrow and Guinle [41], Lin [42], Kuiken [43], and Oosthuizen and Donaldson [44]. Latter, Na and Chiou [45-46] studied the laminar natural convection flow over a frustum of a cone. They included the constant wall temperature as well as the constant wall heat flux cones in the thermal boundary conditions at the wall. Alamgir [47] used an integral method to study the over-all heat transfer from vertical cones in laminar natural convection. Recently, Hossain and Paul [48] have investigated the natural convection flow from a heated vertical permeable circular cone. The solutions were obtained against the local variable ξ that represents the streamwise distribution of the transpiration velocity.

Radiative convective flows are encountered in many industrial and environmental processes e.g. heating and cooling chambers, fossil fuel combustion energy processes, evaporation from large open water reservoirs, astrophysical flows, solar power technology and space vehicle re-entry. Mathematically the equations for radiative heat transfer with absorption, scattering and emission can be generated by one of two approaches, namely the continuum model or the spectral radiative treatment of a single particle. Details of the derivation of the general equation of radiative heat transfer are provided in the classic monograph by Chandrasekhar [7].

Little is currently known about the boundary layer flows of radiating fluids. The inclusion of conduction-radiation effects in the energy equation, however, leads to a more highly nonlinear partial differential equation. The majority of studies concerned with the interaction of thermal radiation and natural convection were made by Sparrow and Cess [29], Cess [4], Arpaci [1], Cheng and Ozisik [5], Hasegawa et al. [16], and Bankston et al. [2] for the case of a vertical semi-infinite plate. In recent years, Soundalgekar and Takhar [26] have studied radiation effects on free convection flow of a gas past a semi-infinite flat plate using Cogley-Vincontine-Giles equilibrium model (Cogley et al., [6]) and Hossain and Takhar [19] have analyzed

the effect of radiation using the Rosseland diffusion approximation which leads to a nonsimilar mixed convective boundary-layer flow of an optically dense viscous incompressible fluid past a heated vertical plate with a uniform free stream velocity and surface temperature. The boundary layer equations were obtained using a group of transformations and they are valid in both the forced convective and free convective limits. The resulting equations were solved using an implicit finite difference method. Recently the problem of natural convection-radiation interaction on boundary layer flows with the Rosseland diffusion approximation been studied by Hossain and Alim [20] and Hossain et al. [21]; and very recently, Hossain and Rees [23] have investigated the effect of radiation–conduction interaction in the mixed convective flow along a slender impermeable vertical cylinder. M. Kutubuddin, M. A. Hossain and I. Pop [33,27] analyze the effect of conduction-radiation interaction on the forced, free and mixed convection flow from a horizontal cylinder

The inclusion of radiation term is complicated and the resulting equations are very difficult to solve. Grief and Habib [17] have shown that, in the optically thin limit, the physical situation can be simplified and they derived an exact solution of the problem of fully-developed radiating laminar convection flow in an infinite vertical heated channel. Their analysis was based on the work by Cogley et al. [6]. In the optically thin limit the fluid does not absorb its own emitted radiation but the fluid does absorb radiation emitted by the boundaries. It was shown by Cogley et al. [6] that in optically thin limit for a gray-gas near equilibrium, the following relation holds:

$$\frac{\partial q_r}{\partial y} = 4(T - T_w) \int_0^\infty \kappa_{\lambda w} \left(\frac{\partial e_{b\lambda}}{\partial T} \right)_w d\lambda = 4(T - T_w)I ,$$

where $I = \int_0^\infty \kappa_{\lambda w} \left(\frac{\partial e_{b\lambda}}{\partial T} \right)_w d\lambda$.

Here q_r is the radiative flux, κ_λ is the absorption coefficient, $e_{b\lambda}$ is the Planck function and the subscript w, represents the value of a quantity at the wall. Further simplification may be made concerning the spectral properties of radiating gases, but this is not essential for the present analysis. It should be mentioned that

Soundalgekar and Takhar [28] have considered the radiative free convective flow of an optically thin grey -gas past a semi-infinite vertical plate.

But, the Rosseland model is valid for isotropic local intensity and high optical density of the medium and the radiative heat flux is given by

$$q_r = -\frac{16\sigma\nabla T^3}{3(a_R + \sigma_s)}\nabla T$$

where T denotes the temperature, a_R is the Rosseland absorption coefficient, σ_s is the scattering coefficient and σ is the Stefan-Boltzmann constant [7]. The thermal boundary-layer equation can be written as

$$\rho C_p\left(u\frac{\partial T}{\partial x} + v\frac{\partial T}{\partial y}\right) = \frac{\partial}{\partial y}\left[\left(\frac{16\sigma T^3}{3a_R} + \kappa\right)\frac{\partial T}{\partial y}\right]$$

Here we have considered in detail how the combined effects of surface radiation and sinusoidal surface temperature profiles in the streamwise direction modify the otherwise self-similar boundary-layer flow. Solutions are presented in terms of the surface rate of heat transfer and shear stress and detailed isotherms are also given. An important feature of the flow is that a near-wall layer develops at large distances down-stream of the leading edge. The numerical evidence suggests that this inner layer decreases in thickness with distance down-steam. A finite difference method was employed in obtaining the numerical solutions. The effect of varying different physical parameters on the local skin-friction and local rate of heat transfer are presented.

8

Chapter 2

Governing equations and boundary-layer analysis

We consider the boundary layer induced by a heated semi-infinite surface immersed in an incompressible Newtonian fluid. In particular, the heated surface is maintained at the steady temperature.
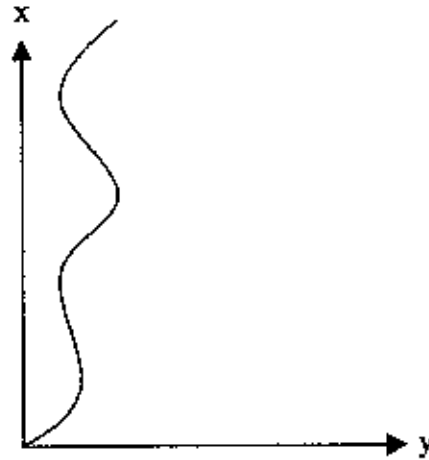

Fig: The flow configuration

$$T = T_\infty + (T_w - T_\infty)(1 - a\sin(\pi\hat{x}/d)) \tag{2.1}$$

where T_∞ is the ambient fluid temperature, T_w is the mean-surface temperature which is such that $T_w > T_\infty$, a is the relative amplitude of the surface temperature variations and 2d is the wavelength of the variations. The steady two-dimensional equations of motion are given by

$$\hat{u}_x + \hat{v}_y = 0 \tag{2.2}$$

$$\hat{u}\hat{u}_x + \hat{v}\hat{u}_y = -\frac{1}{\rho}\hat{p}_x + Gr^{1/2}(\hat{u}_{xx} + \hat{u}_{yy}) + T - T_\infty \tag{2.3}$$

$$\hat{u}\hat{v}_x + \hat{v}\hat{v}_y = -\frac{1}{\rho}\hat{p}_y + Gr^{-1/2}(\hat{v}_{xx} + \hat{v}_{yy}) \tag{2.4}$$

$$\hat{u}T_x + \hat{v}T_y = \frac{1}{Pr}Gr^{-1/2}\left[T_{yy} + \frac{16\sigma}{3\kappa(a + \sigma_s)}\{T^3 T_y\}_y\right] \tag{2.5}$$

9

Boundary conditions are

$$\hat{u} = 0, \quad \hat{v} = 0, \quad T = T_\infty + (T_w - T_\infty)(1 + a\sin\pi\tfrac{\hat{x}}{L}) \quad \text{at} \quad \hat{y} = 0$$

$$\hat{u} = 0, \quad T = T_\infty \quad \text{as} \quad \hat{y} \to \infty$$

where Gr is the Grashof number and Pr. is the Prandtl number. In the derivation of equations (2.2) the Boussinesq approximation has been assumed. We note that the Grashof number has been based on d, half the dimensional wavelength of the thermal waves.

In the equations, u and v are, respectively, the velocity components in the x and y directions, T is the fluid temperature, ν is the kinematic viscosity, β is the thermal expansion coefficient, α is the thermal diffusivity, κ is the thermal conductivity , a is the Rosseland mean absorption coefficient, σ is the Stephan-Boltzman constant, σ_s is the scattering coefficient.

When the surface temperature is uniform and the Grashof number is very large, the resulting boundary-layer flow is self-similar. But the presence of sinusoidal surface temperature distributions, such as that given by (2.1), renders the boundary-layer flow non-similar. The boundary-layer equations are obtained by introducing the scaling

$$u = \frac{L}{\nu}Gr^{-\frac{1}{2}}\hat{u}, \quad v = \frac{L}{\nu}Gr^{-\frac{1}{4}}\hat{v}, \quad x = \frac{\hat{x}}{L},$$

$$y = \frac{\hat{y}}{L}Gr^{\frac{1}{4}}, \quad p = \frac{L^2}{\rho\nu^2}Gr^{-1}\hat{p}, \quad \theta = \frac{T-T_\infty}{T_w-T_\infty} \tag{2.6}$$

into equations (2.3)-(2.5), formally letting Gr becomes asymptotically large and retaining only the leading order terms. Thus we obtain

$$u_x + v_y = 0 \tag{2.7}$$

$$uu_x + vu_y = u_{yy} + \theta \tag{2.8}$$

$$uv_x + vv_y = -p_y + v_{yy} \tag{2.9}$$

$$u\theta_x + v\theta_y = \frac{1}{\text{Pr}}\left[\theta_{yy} + \frac{16\sigma}{3\kappa(a+\sigma_s)}\left\{\theta^3\theta_y\right\}_y\right] \tag{2.10}$$

where the asterisk superscripts have been omitted for clarity of presentation. Equation (2.9) serves to define the pressure field in terms of the two velocity components and is decoupled from the other three equations. Therefore, we shall not consider it further. As the equations are two-dimensional we define a stream function ψ, in the usual way.

$$u = \psi_y, \quad v = -\psi_x \tag{2.11}$$

and therefore, (2.7) is satisfied automatically. Guided by the familiar self-similar form corresponding to a uniform surface temperature, we use the substitution

$$\psi = x^{3/4} f(\eta, x), \quad \theta = g(\eta, x) \tag{2.12}$$

where

$$\eta = y / x^{1/4} \tag{2.13}$$

is the pseudo-similarity variable. Equation (2.8) and (2.9) reduce to

$$f''' + g + \tfrac{3}{4}ff'' - \tfrac{1}{2}ff' + x(f_x f'' - f_x f') = 0 \tag{2.14}$$

$$\frac{1}{\text{Pr}}\left[\left\{1 + \frac{4}{3}R_d\left(1 + (\theta_w - 1)g\right)^3\right\}g'\right]' \tag{2.15}$$

$$+ \tfrac{3}{4}fg' + x(f_x g' - fg_x) = 0$$

and the boundary conditions are

$$f = 0, \quad f' = 0, \quad g = 1 + a\sin\pi x$$

$$\text{at } \eta = 0 \text{ and } fg \to 0 \text{ as } \eta \to \infty. \tag{2.16}$$

In equations (2.14)-(2.16), primes denote derivatives with respect to η.

Chapter 3

Finite difference method and asymptotic analysis

In our analysis, we have employed a number of methods for the numerical solution of the differential equations. Of them the most practical, efficient and accurate solution technique is implicit finite difference method together with Keller-box elimination technique, which is well-documented and widely used by Keller-box and Cebeci [24] and recently by Hossain [48].

$$f''' + \frac{3}{4} ff'' - \frac{1}{2} f'^2 + g = x \left(f' \frac{\partial f}{\partial x} - f'' \frac{\partial f}{\partial x} \right)$$

(3.1)

To apply the aforementioned method, we first convert the momentum Eqs. (3.1) into the following system of first order equations with dependent variables, $u(\xi,\eta), \; v(\xi,\eta)$ as

$$f' = u$$ (3.2a)

$$u' = v$$ (3.2b)

$$v' + \frac{3}{4} fv - \frac{1}{2} u^2 + g = \xi \left(u \frac{\partial u}{\partial \xi} - v \frac{\partial f}{\partial \xi} \right)$$ (3.2c)
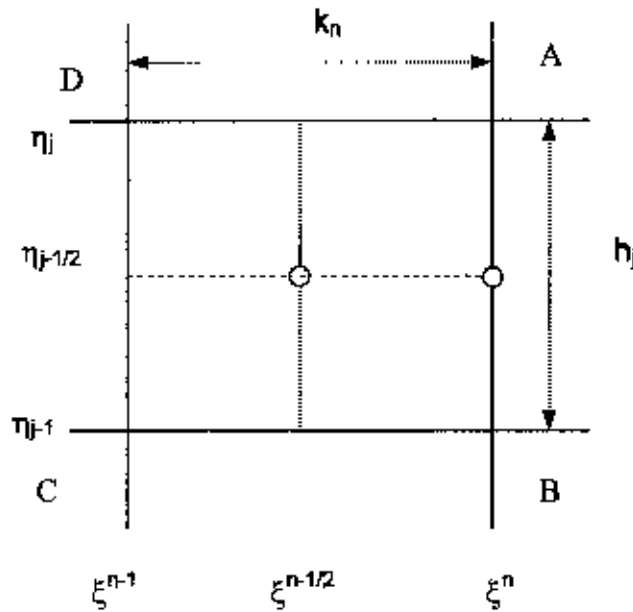
where $x = \xi$

and the boundary conditions are

$$f(\xi,0) = 0, \; u(\xi,0) = 0, \; g(\xi,0) = 1 + a \sin \pi \xi$$

(3.3)

We now consider the net rectangle on the (ξ,η) plane and denote the net points by

$$\eta_0 = 0, \ \eta_j = \eta_{j-1} + h_j, \ j = 1, 2, \cdots, J$$
$$\xi^0 = 0, \ \xi^n = \xi^{n-1} + k_n, \ n = 1, 2, \cdots, N \tag{3.4}$$

Here n and j are just sequence of numbers on the (ξ, η) plane, k_n and h_j be the variable mesh widths.

Fig. 1 Net rectangle of the difference approximation

We approximate the quantities (f, u, v, g) at the point (ξ^n, η_j) of the net by $(f_j^n, u_j^n, v_j^n, g_j^n)$, which we call net function. We also employed the notation g_j^n for the quantities midway between net points shown in figure 1 and for any net function as

$$\xi^{\frac{n-1}{2}} = \frac{1}{2}(\xi^n + \xi^{n-1}) \tag{3.5a}$$

13

$$\eta_{\frac{j-1}{2}} = \frac{1}{2}(\eta_j + \eta_{j-1}) \tag{3.5b}$$

$$g_j^{\frac{n-1}{2}} = \frac{1}{2}(g_j^n + g_j^{n-1}) \tag{3.5c}$$

$$g_{j-1/2}^n = \frac{1}{2}(g_j^n + g_{j-1}^{n-1}) \tag{3.5d}$$

Now we write the difference equations that are to approximate Eqs. (3.5a)-(3.5d) by considering one mesh rectangle for the mid point $\left(\xi^n, \eta_{j-1/2}\right)$ to obtain

$$\frac{f_j^n - f_{j-1}^n}{h_j} = u_{j-1/2}^n \tag{3.6a}$$

$$\frac{u_j^n - u_{j-1}^n}{h_j} = v_{j-1/2}^n \tag{3.6b}$$

Similarly Eqs. (3.6a)-(3.6b) are approximated by centering about the mid point $\left(\xi^{n-1/2}, \eta_{j-1/2}\right)$. Centering the Eq.(3.6a) about the point $\left(\xi^{n-1/2}, \eta\right)$ without specifying η to obtain the algebraic equations. If we denote the left hand side of eq.(3.2c) by L, then the difference approximation to eq. (3.2c) is

$$\frac{1}{2}(L^n + L^{n-1}) = \xi^{n-\frac{1}{2}}\left[u^{n-\frac{1}{2}}(\frac{u^n - u^{n-1}}{k_n}) - v^{n-\frac{1}{2}}(\frac{f^n - f^{n-1}}{k_n}) \right] \tag{3.7}$$

where

$$L^n = \left[v' + \frac{3}{4}fv - \frac{1}{2}u^2 + g \right]^n$$

and

14

$$L^{n-1} = \left[v' + \frac{3}{4} fv - \frac{1}{2} u^2 + g \right]^{n-1}$$

$$\left[v' \right]^n + \alpha_1 (fv)^n - \alpha_2 \left(u^2 \right)^n + \alpha \left[v^{n-1} f^n - v^n f^{n-1} \right] + g^n = R^{n-1} \tag{3.8}$$

where

$$R^{n-1} = -L^{n-1} + \alpha \left[(fv)^{n-1} - \left(u^2 \right)^{n-1} \right]$$

$$\alpha = \frac{\xi^{n-\frac{1}{2}}}{k_n}$$

$$\alpha_1 = \frac{3}{4} + \alpha$$

$$\alpha_2 = \frac{1}{2} + \alpha$$

Now we take position at $\eta = \eta_{j-\frac{1}{2}}$ then eq.(3.8) becomes

$$\left[v' \right]^n_{j-\frac{1}{2}} + \alpha_1 (fv)^n_{j-\frac{1}{2}} - \alpha_2 \left(u^2 \right)^n_{j-\frac{1}{2}}$$

$$+ \alpha \left[v^{n-1}_{j-\frac{1}{2}} f^n_{j-\frac{1}{2}} - v^n_{j-\frac{1}{2}} f^{n-1}_{j-\frac{1}{2}} \right] + g^n_{j-\frac{1}{2}} = R^{n-1}_{j-\frac{1}{2}} \tag{3.9}$$

where

$$R^{n-1}_{j-\frac{1}{2}} = -L^{n-1}_{j-\frac{1}{2}} + \alpha \left[(fv)^{n-1}_{j-\frac{1}{2}} - \left(u^2 \right)^{n-1}_{j-\frac{1}{2}} \right]$$

and

$$L^{n-1}_{j-\frac{1}{2}} = h_j^{-1} \left(v_j^{n-1} - v_{j-1}^{n-1} \right) + \frac{3}{4} (fv)^{n-1}_{j-\frac{1}{2}} - \frac{1}{2} \left(u^2 \right)^{n-1}_{j-\frac{1}{2}} + g^{n-1}_{j-\frac{1}{2}}$$

Eqn. (3.8) becomes

$$h_j^{-1}\left[v_j^n - v_{j-1}^n\right] + \alpha_1 (fv)_{j-\frac{1}{2}}^n - \alpha_2 \left(u^2\right)_{j-\frac{1}{2}}^n + g_{j-\frac{1}{2}}^n$$

$$+ \alpha\left(v_{j-\frac{1}{2}}^{n-1} f_{j-\frac{1}{2}}^n - v_{j-\frac{1}{2}}^n f_{j-\frac{1}{2}}^{n-1}\right) = R_{j-\frac{1}{2}}^{n-1} \qquad (3.10)$$

The boundary conditions reduce to the following form

$$f_0^n = 0, \quad u_0^n = 0, \quad g_0^n = 1 + a \sin \pi \xi \qquad (3.11)$$

Finally we get

$$h_j^{-1}\left(f_j^n - f_{j-1}^n\right) = u_{j-\frac{1}{2}}^n \qquad (3.12a)$$

$$h_j^{-1}\left(u_j^n - u_{j-1}^n\right) = v_{j-\frac{1}{2}}^n \qquad (3.12b)$$

$$h_j^{-1}\left(v_j^n - v_{j-1}^n\right) + \alpha_1 (fv)_{j-\frac{1}{2}}^n - \alpha_2 \left(u^2\right)_{j-\frac{1}{2}}^n + g_{j-\frac{1}{2}}^n$$

$$+ \alpha\left(v_{j-\frac{1}{2}}^{n-1} f_{j-\frac{1}{2}}^n - v_{j-\frac{1}{2}}^n f_{j-\frac{1}{2}}^{n-1}\right) = R_{j-\frac{1}{2}}^{n-1} \qquad (3.12c)$$

We define the iterates

$$\left[f_j^{(i)}, \ u_j^{(i)}, \ v_j^{(i)}, \ g_j^{(i)}\ \right] \ j = 1, 2 \ldots$$

with initial values equal to those at the previous ξ station (which is usually the best initial guess variables). For higher iterates we get

$$f_j^{(i+1)} = f_j^{(i)} + \delta f_j^{(i)} \qquad (3.13a)$$

16

$$u_j^{(i+1)} = u_j^{(i)} + \delta\, u_j^{(i)} \tag{3.13b}$$

$$v_j^{(i+1)} = v_j^{(i)} + \delta\, v_j^{(i)} \tag{3.13c}$$

$$g_j^{(i+1)} = g_j^{(i)} + \delta\, g_j^{(i)} \tag{3.13d}$$

Now we insert the right hand side of the expression in place of f_j, u_j, v_j, g_j in eqs. (3.12a)-(3.12b) and drop the terms that are quadratic in

$$\delta\, f_j^{(i)}, \quad \delta\, u_j^{(i)}, \quad \delta\, v_j^{(i)}, \quad \delta\, g_j^{(i)}$$

to yield the following linear system (for simplicity, the subscript i in δ quantities is dropped)

$$\delta f_j - \delta f_{j-1} - \frac{h_j}{2}\left(\delta u_j + \delta u_{j-1}\right) = \left(r_1\right)_j \tag{3.14a}$$

$$\delta u_j - \delta u_{j-1} - \frac{h_j}{2}\left(\delta v_j + \delta v_{j-1}\right) = \left(r_3\right)_j \tag{3.14b}$$

$$\left(S_1\right)_j \delta v_j + \left(S_2\right)_j \delta v_{j-1} + \left(S_3\right)_j \delta f_j + \left(S_4\right)_j \delta f_{j-1} + \left(S_5\right)_j \delta u_j$$
$$+ \left(S_6\right)_j \delta u_{j-1} + \left(S_7\right)_j \delta g_j + \left(S_8\right)_j \delta g_{j-1} = \left(r_2\right)_j \tag{3.14c}$$

where

$$\left(r_1\right)_j = f_{j-1}^{(i)} - f_j^{(i)} + h_j u_{j-\frac{1}{2}}^{(i)} \tag{3.15a}$$

$$\left(r_4\right)_j = u_{j-1}^{(i)} - u_j^{(i)} + h_j v_{j-\frac{1}{2}}^{(i)} \tag{3.15b}$$

$$\left(r_2\right)_j = R_{j-\frac{1}{2}}^{n-1} - h_j^{-1}\left(v_j' - v_{j-1}'\right) + \alpha_1 \left(fv\right)_{j-\frac{1}{2}} - \alpha_2 \left(u^2\right)_{j-\frac{1}{2}} + g_{j-\frac{1}{2}}'$$
$$+ \alpha\left(v_{j-\frac{1}{2}}^{n-1} f_{j-\frac{1}{2}}^{i} - v_{j-\frac{1}{2}}^{i} f_{j-\frac{1}{2}}^{n-1}\right) \tag{3.15c}$$

17

The coefficients of momentum equation are

$$(S_1)_j = h_j^{-1} + \frac{\alpha_1}{2} f_j^{(i)} - \frac{\alpha}{2} f_{j-\frac{1}{2}}^{n-1} \tag{3.15d}$$

$$(S_2)_j = -h_{j-1}^{'} + \frac{\alpha_1}{2} f_{j-1}^{(i)} - \frac{\alpha}{2} f_{j-\frac{1}{2}}^{n-1} \tag{3.15e}$$

$$(S_3)_j = \frac{\alpha_1}{2} v_j^{(i)} + \frac{\alpha}{2} v_{j-\frac{1}{2}}^{n-1} \tag{3.15f}$$

$$(S_4)_j = \frac{\alpha_1}{2} v_{j-1}^{(i)} + \frac{\alpha}{2} v_{j-\frac{1}{2}}^{n-1} \tag{3.15g}$$

$$(S_5)_j = -\alpha_2 u_j^{(i)} \tag{3.15h}$$

$$(S_6)_j = -\alpha_2 u_{j-1}^{(i)} \tag{3.15h}$$

$$(S_7)_j = 0.0 \tag{3.15i}$$

$$(S_8)_j = 0.0 \tag{3.15j}$$

Now for energy equation

$$\frac{1}{\Pr}\left[\left\{1 + \frac{4}{3} R_d \left(1 + (\theta_w - 1)g\right)^3\right\}g'\right]' + \tfrac{3}{4} fg' + x(f_x g' - f' g_x) = 0$$

Let $Rdd = \dfrac{4}{3} R_d$ and $Tw = (\theta_w - 1)$

In the similar way as mentioned above the coefficients of the energy equation are

$$(b_1)_j = \frac{1}{\mathrm{Pr}} h_j^{-1} \left[1 + Rdd(1 + 3Tw\ g'_j + 3Tw^2 g'^2_j + Tw^3 g'^3_j \right] \tag{3.16a}$$

$$+ \frac{K_1}{2} f_j^{(i)} - \frac{K}{2} f_{j-\frac{1}{2}}^{n-1}$$

$$(b_2)_j = -\frac{1}{\mathrm{Pr}} h_j^{-1} \left[\begin{array}{l} 1 + Rdd(1 + 3Tw\ g'_{j-1} \\ + 3Tw^2 g'^2_{j-1} + Tw^3 g'^3_{j-1} \end{array} \right] \tag{3.16b}$$

$$+ \frac{K_1}{2} f_{j-1}^{(i)} - \frac{K}{2} f_{j-\frac{1}{2}}^{n-1}$$

$$(b_3)_j = \frac{\alpha_1}{2} p_j^{(i)} + \frac{\alpha}{2} p_{j-\frac{1}{2}}^{n-1} \tag{3.16c}$$

$$(b_4)_j = \frac{\alpha_1}{2} p_{j-1}^{(i)} + \frac{\alpha}{2} p_{j-\frac{1}{2}}^{n-1} \tag{3.16d}$$

$$(b_5)_j = -\frac{\alpha}{2} g_j^{(i)} + \frac{\alpha}{2} g_{j-\frac{1}{2}}^{n-1} \tag{3.16e}$$

$$(b_6)_j = -\frac{\alpha}{2} g_{j-1}^{(i)} + \frac{\alpha}{2} g_{j-\frac{1}{2}}^{n-1} \tag{3.16f}$$

$$(b_7)_j = -\frac{K}{2}(u'_j + u_{j-\frac{1}{2}}^{n-1}) + 3\frac{Rdd}{\mathrm{Pr}} p_j'^2 (1 + 2Tw\ g'_j + Tw^2 g'^2_j) h_j^{-1} \tag{3.16g}$$

$$(b_8)_j = -\frac{K}{2}(u_{j-1}^i + u_{j-\frac{1}{2}}^{n-1}) + 3\frac{Rdd}{\mathrm{Pr}} p_{j-1}'^2 (1 + \tag{3.16h}$$

$$2Tw\ g'_{j-1} + Tw^2 g'^2_{j-1}) h_j^{-1}$$

$$(b_9)_j = 0.0 \tag{3.16i}$$

$$(b_{10})_j = 0.0 \tag{3.16j}$$

Asymptotic Analysis

The momentum and energy equations are

$$f''' + g + \tfrac{3}{4} ff'' - \tfrac{1}{2} ff' + x(f_x f'' - f_x f') = 0 \tag{3.17}$$

$$\frac{1}{Pr}\left[\left\{1 + \frac{4}{3} R_d (1 + (\theta_w - 1)g)^3\right\}g'\right]' + \tfrac{3}{4} fg' + x(f_x g' - f g_x) = 0 \tag{3.18}$$

For simplicity let $\alpha_1 = \dfrac{4}{3} R_d, \ \alpha_2 = \theta_w - 1$

Then eq. (3.18) becomes

$$\frac{1}{Pr}\left[\left\{1 + \alpha_1 (1 + \alpha_2 g)^3\right\}g'\right]' + \tfrac{3}{4} fg' + x(f_x g' - f g_x) = 0 \tag{3.19}$$

And the boundary conditions are

$$f = 0, \quad f' = 0, \quad g = 1 + a \sin \pi x$$

at $\eta = 0$ and $f, g \to 0$ as $\eta \to \infty$. $\tag{3.20}$

Following Rees (1999) the boundary layer looks like the uniform case (a=0) at the leading order in the main part of the flow (i.e. not near the surface. Therefore set $f \sim f_0(\eta)$ and $g \sim g_0(\eta)$ where $f_0 \& g_0$ satisfy the following equations

$$f_0''' + g_0 + \tfrac{3}{4} f_0 f_0'' - \tfrac{1}{2} f_0' f_0' = 0 \tag{3.21}$$

$$\frac{1}{Pr}\left[\left\{1 + \alpha_1 (1 + \alpha_2 g)^3\right\}g'\right]' + \tfrac{3}{4} fg' + x(f_x g' - f g_x) = 0 \tag{3.22}$$

20

Subject to the boundary conditions

$$f = 0, \quad f' = 0, \quad g = 1 + a\sin \pi x \qquad (3.23)$$

at $\eta = 0$ and $fg \to 0$ as $\eta \to \infty$.

We need to look near to $\eta = 0$ to account for the variation in g there. We need a Taylor Series representation of f_0 & g_0:

$$f_0 = \frac{1}{2}a_2\eta^2 - \frac{1}{6}\eta^3 + \cdots \qquad (3.24)$$

$$g_0 = 1 + b_1\eta + \cdots \qquad (3.25)$$

where

$$a_2(\mathrm{Pr}, R_d, \theta_w) = a_2(\mathrm{Pr}, \alpha_1, \alpha_2) = f_0''(0) > 0$$
$$b_1 = g_0'(0) < 0$$

To find the scaling for the inner region we need to balance f''' (highest derivative), g (buoyancy term which drives the flow) and $x(f_x f'' - f_x' f')$ (which mediates the boundary temperature effect). This process is more stable than is usual for such problems.

From (3.24) we obtain

$$\frac{d^3 f}{d\eta^3} = O(1) \Rightarrow f = O(\eta^{-3})$$
$$g = O(1)$$
$$xf_x f'' = O(xf)$$

Hence $\eta = O(x^{-\frac{1}{3}})$ and $f = O(x^{-1})$. However, we note that $f'' = O(1)$ in (3.20)

and these scaling should give $f'' = O(x^{-\frac{1}{3}})$ the resolution comes from the fact that

the $O(\eta^2)$ term in (3.20) is transmitted passively into the inner layer without modification.

In the inner layer we let $f = F(\xi, x)$ $g = G(\xi, x)$ where $\xi = \eta x^{\frac{1}{3}}$ from our scaling. Hence

$$\frac{\partial}{\partial \eta} \to x^{\frac{1}{3}} \frac{\partial}{\partial \xi}, \qquad \frac{\partial}{\partial x} = \frac{\partial}{\partial x} + \frac{1}{3} \frac{\xi}{x} \frac{\partial}{\partial \xi} \tag{3.26}$$

and equations (3.17) & (3.18) become

$$F''' + x^{-\frac{1}{3}}(\tfrac{3}{4}FF'' - \tfrac{5}{6}F'F') + x^{-1}G + x^{\frac{2}{3}}(F_x F'' - F_x' F') = 0 \tag{3.27}$$

$$\frac{1}{\mathrm{Pr}}\left[\{1 + \alpha_1(1 + \alpha_2 G)^3\}G'' + 3\alpha_1\alpha_2(1 + \alpha_2 G)^2 G'G' \right] \tag{3.28}$$

$$+ \tfrac{3}{4}x^{-\frac{1}{3}}FG' + x^{\frac{2}{3}}(F_x G' - F'G_x) = 0$$

Guided by the scaling analysis and by (3.20), we set

$$F = x^{-\frac{2}{3}}F_0 + x^{-1}F_1 + \cdots$$
$$G = G_0 + x^{-\frac{1}{3}}G_1 + \cdots \tag{3.29}$$

into (3.23) and (3.24) to get

$$f = f_0(\eta) + x^{-\frac{1}{3}}f_1 + x^{-\frac{2}{3}}f_2 + \cdots$$
$$g = g_0(\eta) + x^{-\frac{1}{3}}g_1 + x^{-\frac{2}{3}}g_2 + \cdots \tag{3.30}$$

22

where $F \neq F' \neq 0$, $G = 1 + a \sin \pi x$ at $\xi = 0$

and F & G match with f & g as $\xi \to \infty$ and $\eta \to 0$.

Inner region leading order

Equation for F_0 is

$$F_0''' = 0$$

Solution of this equation must be

$$F_0 = \frac{1}{2} a_2 \xi^2 \tag{3.31}$$

which satisfies $F_0 = F_0' = 0$ at $\xi = 0$ and the small η matching condition from (3.20)

Equation for G_0 is

$$\frac{1}{Pr}\left[\left\{1 + \alpha_1(1 + \alpha_2 G)^3\right\}G'' + 3\alpha_1\alpha_2(1 + \alpha_2 G)^2 G'G'\right] + F_{0x}G_0' - F_0'G_{0x}) = 0 \tag{3.32}$$

Using (3.27) we have

$$\frac{1}{Pr}\left[\left\{1 + \alpha_1(1 + \alpha_2 G)^3\right\}G'' + 3\alpha_1\alpha_2(1 + \alpha_2 G)^2 G'G'\right] - a_2\xi G_{0x} = 0 \tag{3.33}$$

Subject to

$$G_0 = 1 + a \sin \pi x \quad at \quad \xi = 0$$

and $G_0 \to 1$ as $\xi \to \infty$.

Now at this point we obtain the first essential difference between the present problem and Rees(14). Here eq (3.28) is nonlinear where as eq (3.25) reduced (3.22) to ordinary differential form. In this problem we cannot do this and it is essential to solve (3.28) using the Keller Box method using $G_0=1$ at $x=0$, continuing until the solution becomes periodic.

However we also need to obtain the next term in F in order to recover the leading order effect of boundary temperature variations. From (3.27) we see that it is

$$F_1''' + G_0 + F_0''F_{1x} - F_0'F_{1x}' = 0$$

subject to $F_1 = F_1' = 0$ at $\eta = 0$

and $F_1 \sim -\frac{1}{6}\xi^3$ as $\xi \to \infty$

Hence

$$F_1''' + G_0 + a_2 F_{1x} - a_2 \xi F_{1x}' = 0 \tag{3.34}$$

Probably best to use $F_1'' \to -\xi$ as $\xi \to \infty$ as the matching condition. Therefore we solve (3.28) & (3.34) simultaneously.

Returning to the initial scaling, the rate of heat transfer becomes

$$\left.\frac{\partial g}{\partial \eta}\right|_{\eta=0} = x^{\frac{1}{3}} \left.\frac{\partial G_0}{\partial \xi}\right|_{\xi=0} + \cdots \tag{3.35}$$

and

$$\left.\frac{\partial^2 f}{\partial \eta^2}\right|_{\eta=0} = \left.\frac{\partial^2 F_0}{\partial \xi^2}\right|_{\xi=0} + x^{-\frac{1}{3}}\left.\frac{\partial^2 F_1}{\partial \xi^2}\right|_{\xi=0} = a_2 + x^{-\frac{1}{3}}\left.\frac{\partial^2 F_1}{\partial \xi^2}\right|_{\xi=0} \tag{3.36}$$

To get a second term in the heat transfer expansion we need to go to the next order in the inner layer to obtain:

$$\frac{1}{\text{Pr}}\left[\left\{1+\alpha_1(1+\alpha_2 G_0)^3\right\}G_0'' + 3\alpha_1\alpha_2 G_1 G'' + 6\alpha_1\alpha_2(1+\alpha_2 G_0)^2 G_0' G_1' \\ + 6\alpha_1\alpha_2^2 G_0' G_0' G_1\right]$$

$$+ F_{1x}G_0' - F_0'G_{1x} - F_1'G_{0x}) = 0 \tag{3.37}$$

Subject to $G_1(0) = 0, \quad G_1' \to b_1$

Again, solve with (3.28) and (3.30) until periodicity is obtained. Then

$$\left.\frac{\partial g}{\partial \eta}\right|_{\eta=0} = x^{\frac{1}{3}}\left.\frac{\partial G_0}{\partial \xi}\right|_{\xi=0} + \left.\frac{\partial G_1}{\partial \xi}\right|_{\xi=0} \tag{3.38}$$

Chapter 4

Numerical solutions and discussions

The parabolic system of equations (2.14)-(2.15) together with the boundary conditions (2.16), is non-similar and its numerical solution must be obtained using a marching method. The results presented here were obtained using the Keller-box method, introduced by Keller and Cebeci [24] and described in more detail in Cebeci and Bradshaw [32]. After reduction of equations (2.14)-(2.15) to first-order form in η, the subsequent second-order accurate discretisation based halfway between the grid points in both the η- and x-directions (discussed detailed in Chapter 3) yields a set of nonlinear difference equations which are solved using a multi-dimensional Newton-Raphson iteration scheme. The results presented in Fig. 4.1 to Fig. 4.14 are based on uniform grids in both coordinate directions. There were 201 gridpoints lying between $\eta = 0$ and $\eta = 20$ and 401 between $x = 0$ and $x = 20$. We restrict the presentation of our results to the three values of the Prandtl number: Pr=0.01(Liquid Metal) Pr= 0.7 (air) and Pr = 7 (water).

Fig. 4.1 shows the evolution with x of $f''(\eta = 0)$, a scaled surface shear stress, for constant values of the temperature wave amplitude, a, and the constant radiation parameter R_d for various values of Pr. In this figure we observe that as Pr. is decreasing skin friction is increasing. One point is mentionable that when $Pr.=0.01$, then wave amplitude is higher than that of Pr=7. As x increases, the amplitude of oscillation of the shear stress curves decays slowly.

We observe in Fig. 4.2- Fig.4.4 the evolution with x of surface shear stress, for various values of the temperature wave amplitude, a, and the constant radiation parameter R_d for different values of Pr. In these figure we observe that as Pr is decreasing skin friction is increasing. We also observe that as surface temperature

wave amplitude is increasing shear stress is also increasing, and for decreasing of wave amplitude it is decreasing gradually.

Some aspects of the overall behaviour of these curves may be explained by observing that the boundary layer is thinner when the surface temperature is relatively high and thicker when it is low. These arises because relatively high surface temperatures induce relatively large upward fluid velocities with the consequent increase in the rate of entertainment into the boundary layer. This causes, in turn, a thinning of the boundary layer. Thus, we should expect high shear stresses and rates of heat transfer at, or perhaps just beyond, where the surface temperature attains its maximum values. There is an obvious qualitative difference between the curves shown in Fig. 4.1 and those in Fig. 4.4. As x increases, the amplitude of oscillation of the shear stress curves decays slowly, with x.

Now we want to give our attention to the Fig 4.5 to Fig: 4.7. where the evolution with x of surface shear stress, for constant values of the temperature wave amplitude, a, and the various radiation parameter R_d for different values of Pr. The most interesting part of this analysis is that, when radiation parameter R_d is increasing skin friction is also increasing but when $R_d = 0$. the result of skin friction is exactly the same, which was found by Rees [14]. In our study we have found that skin friction is increasing as R_d is increasing but at a decreasing rate. That is, when $R_d = 1$ then skin friction increases more in respect of $R_d = 10$.

Now we have to analyze the curves, which represents in Fig 4-8 to Fig 4-14, which represents the local Nusselt number that is, the rate of heat transfer.

Fig. 4.8 shows the evolution with x of surface rate of heat transfer, for constant values of the temperature wave amplitude, a, and the constant radiation parameter R_d for various values of Pr. In this figure we observe here that as Pr is decreasing rate of heat transfer increasing. One point is mentionable that when Pr=7.0 (water),

then wave amplitude is higher than that of Pr.=0.01. As x increases, the amplitude of oscillation of the rate of heat transfer increasing significantly.

Here we observe in Fig. 4.9- Fig. 4.11 the evolution with x of surface rate of heat transfer, for various values of the temperature wave amplitude, a, and the constant radiation parameter R_d for different values of Pr. In these figure we observe that as Pr. is decreasing rate of heat transfer increasing. We also observe as surface temperature wave amplitude is increasing rate of heat transfer is also increasing, and for decreasing of wave amplitude it is decreases gradually.

Important aspects of the overall behavior of these curves may be explained by observing that the boundary layer is thinner when the surface temperature is relatively high and thicker when it is low. These arises because relatively high surface temperatures induce relatively large upward fluid velocities with the consequent increase in the rate of entertainment into the boundary layer. This causes, in turn, a thinning of the boundary layer. Thus, we should expect high shear stresses and rates of heat transfer at, or perhaps just beyond, where the surface temperature attains its maximum values. There is an obvious qualitative difference between the curves shown in Fig. 4.8 to Fig. 4.11. As x increases, the amplitude of oscillation of the rate of heat transfer curves increases gradually, with x.

Indeed, the curves in Fig. 4.9 to Fig. 4.11 suggest that, whatever the value of a, there will always be a value of x beyond which some part of the rate of the heat transfer curve between successive surface temperature maxima will be positive. This somewhat unusual phenomenon for boundary layer flows may be explained by noting that when relatively hot fluid encounters a relatively cold part of the heated surface the overall heat transfer will be from the fluid into the surface, rather than the other way around.

Now wa have to give our attention to the figures Fig. 4.12 to Fig.4.14 where the evolution with x of surface rate of heat transfer, for constant values of the

28

temperature wave amplitude, a, and the various radiation parameter R_d for different values of Pr. The most interesting part of this analysis is that, when radiation parameter R_d is increasing rate of heat transfer is also increasing but when R_d =0. the result of rate of heat transfer is exactly the same, which was found by Rees [14]. In our study we have found that rate of heat transfer is increasing as R_d is increasing but at a decreasing rate. That is, when R_d =1 then the rate of heat transfer increased more in respect of R_d =10.

Fig. 4.15 to 4.17 show the isotherms for Pr.=0.7 and $a = 0.2$, for R_d=0.0, 5.0, 10.0. Here we see that the boundary layer maintains its overall thickness in terms of η when x is large, although variations in thickness are clearly present when x is small. The thickness of the region in which strong, surface induced temperature variations are present reduces slowly in size as x increases. It is also clear that isolines are increasing due to increasing of radiation parameter.

In Fig. 4.18 to 4.20 are showing the isotherms for Pr.=7.0 and $a = 0.2$, for R_d=0.0, 5.0, 10.0. Here we see that the boundary layer maintains its overall thickness in terms of η when x is large, although variations in thickness are clearly present when x is small. The thickness of the region in which strong, surface induced temperature variations are present reduces slowly in size as x increases. It is also clear that isolines are increasing due to increasing of radiation parameter.

Presentation of Figure
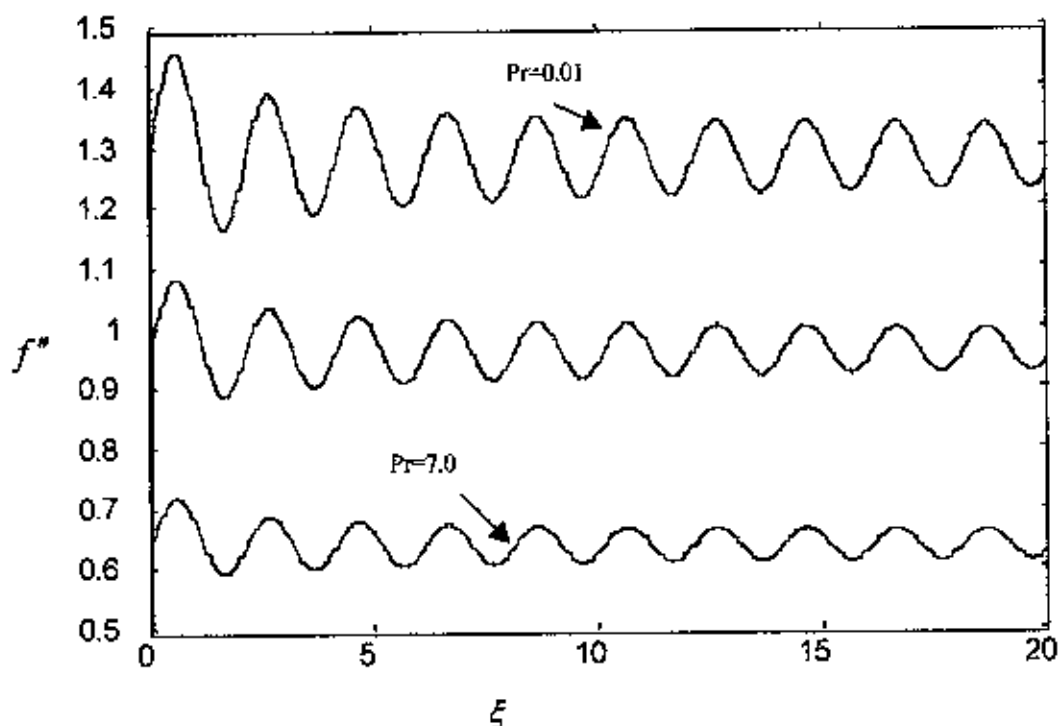
Fig 4.1: Skin friction against ξ for R_d=0.0, a=0.2, Pr.=7.0, 0.7, 0.01.
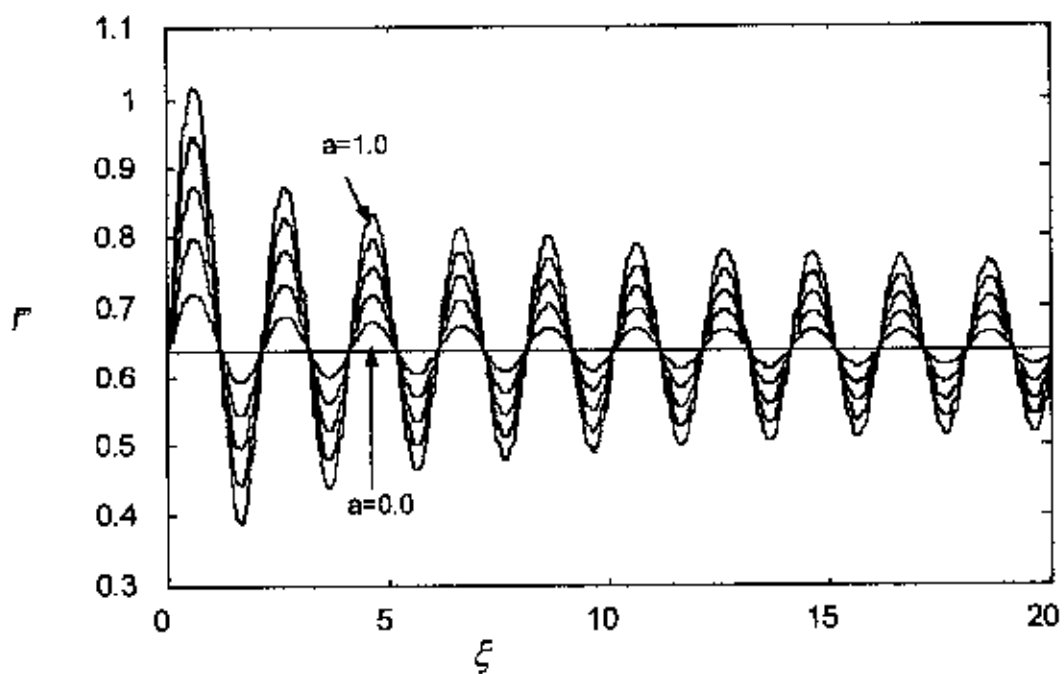
Fig 4.2: Skin friction against ξ for R_d=0.0, a=0.0, 0.2, 0.4, 0.6, 0.8, 1.0 at Pr.=7.0

31
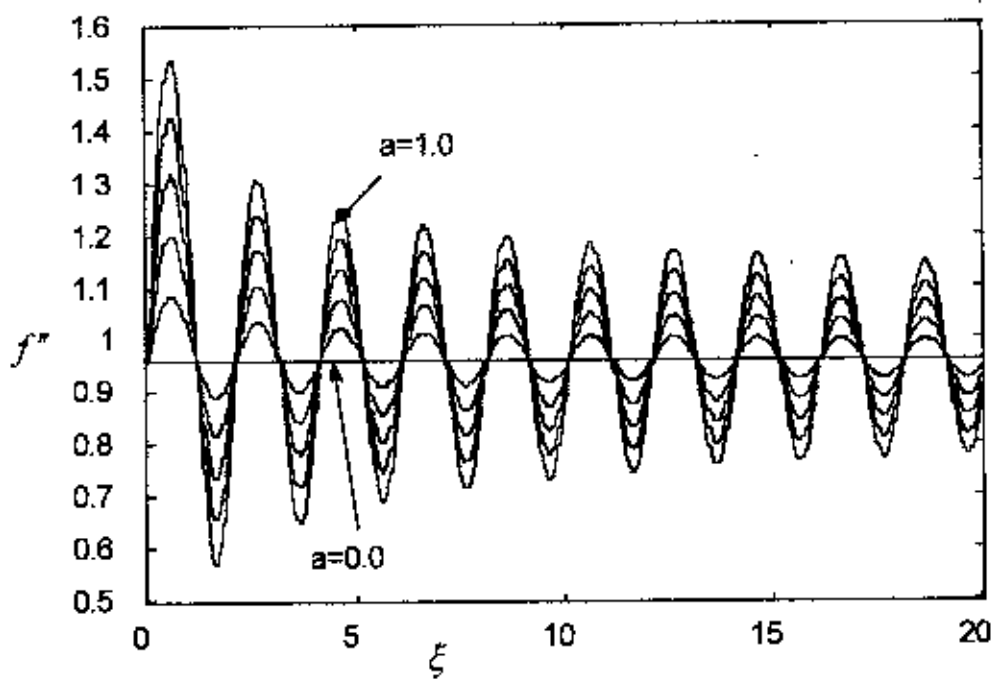
Fig 4.3: Skin friction against ξ for $R_d=0.0$, $a=0.0$, 0.2, 0.4, 0.6, 0.8, 1.0 at Pr.=0.7
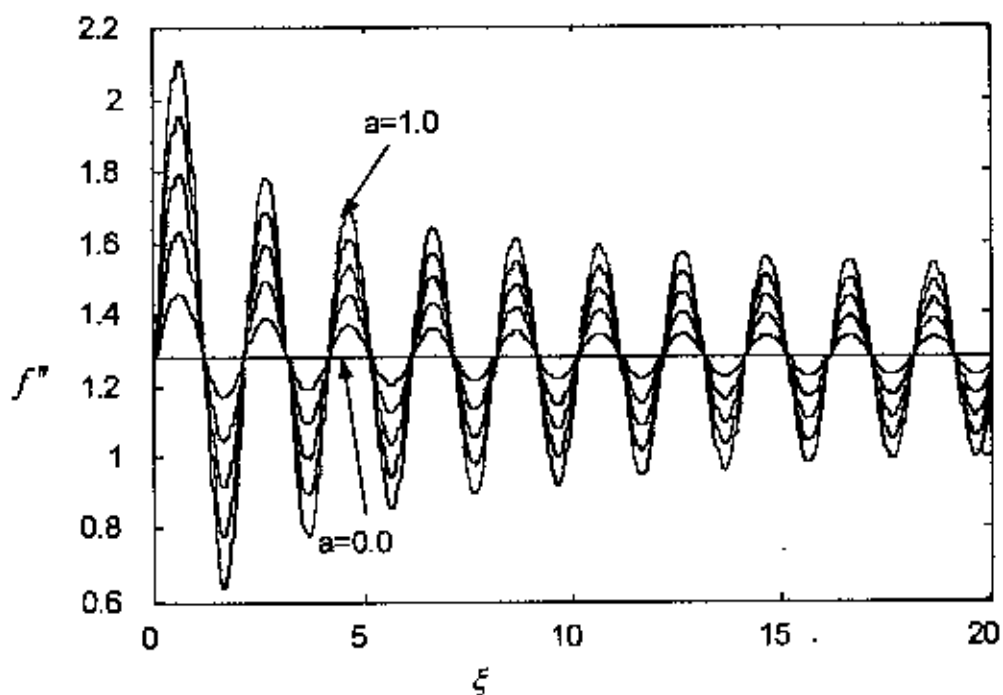
Fig 4.4: Skin friction against ξ for $R_d=0.0$, $a=0.0$, 0.2, 0.4, 0.6, 0.8, 1.0 at Pr.=0.01
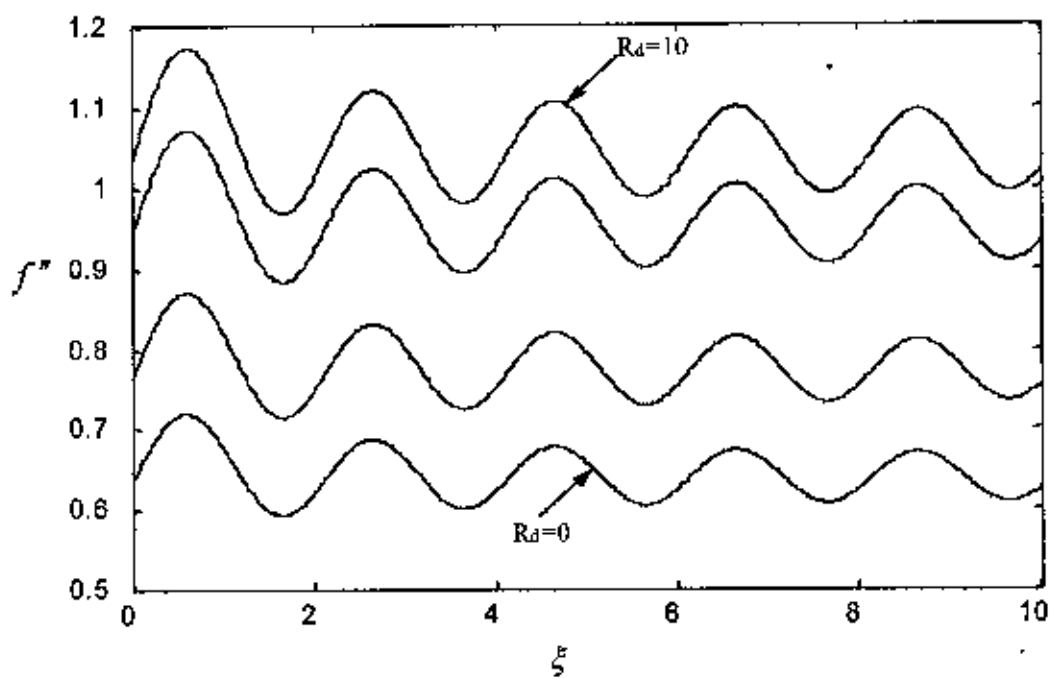
Fig 4.5: Skin friction against ξ for R_d=0.0, 1.0, 5.0, 10.0 a=0.2, at Pr=7.0
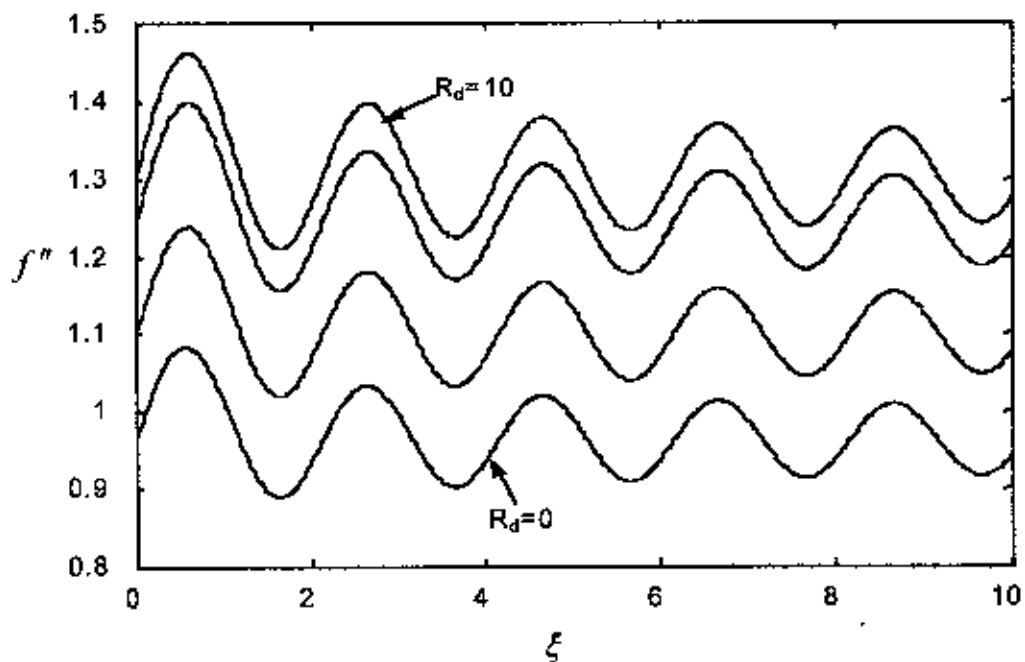
Fig 4.6: Skin friction against ξ for R_d=0.0, 1.0, 5.0, 10.0 a=0.2, at Pr.=0.7

33
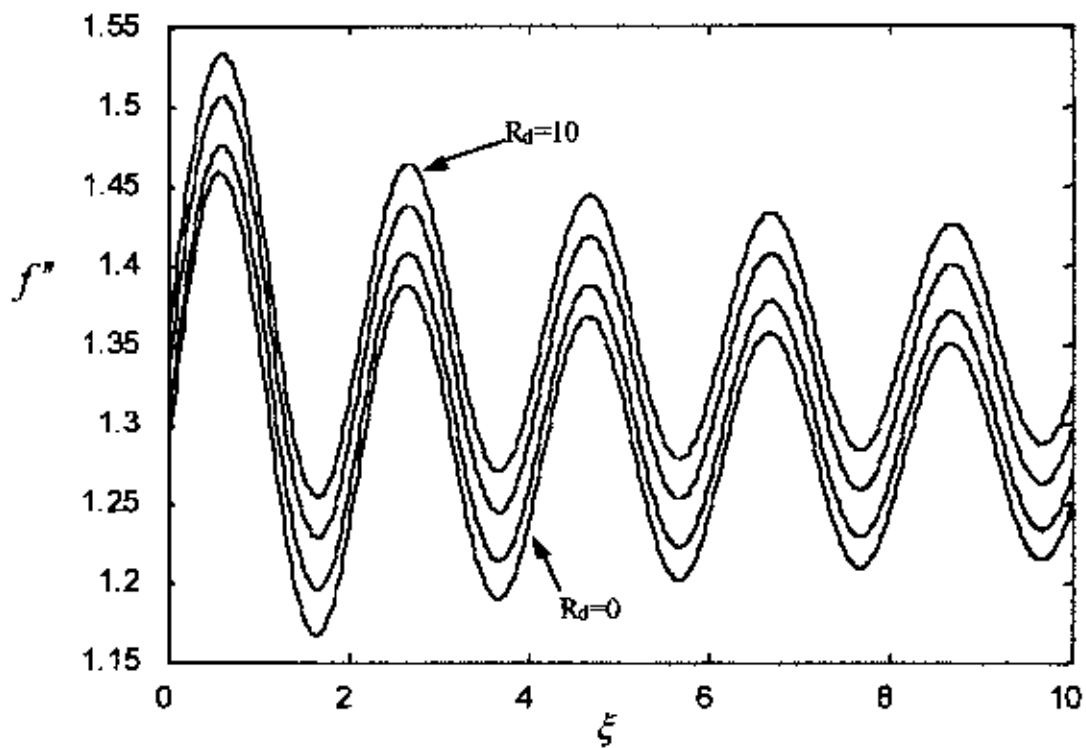
Fig 4.7: Skin friction against ξ for R_d=0.0, 1.0, 5.0, 10.0 a=0.2, at Pr.=0.01
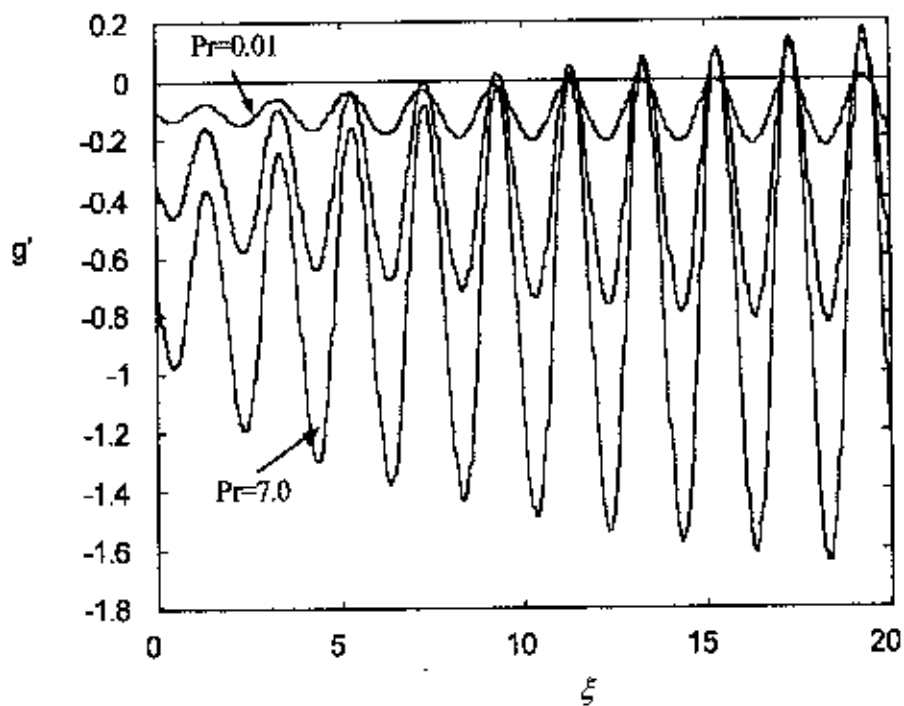
Fig 4.8: Rate of heat transfer against ξ for $R_d=0.0$, $a=0.2$, and Pr.$=7.0$, 0.7, 0.01.
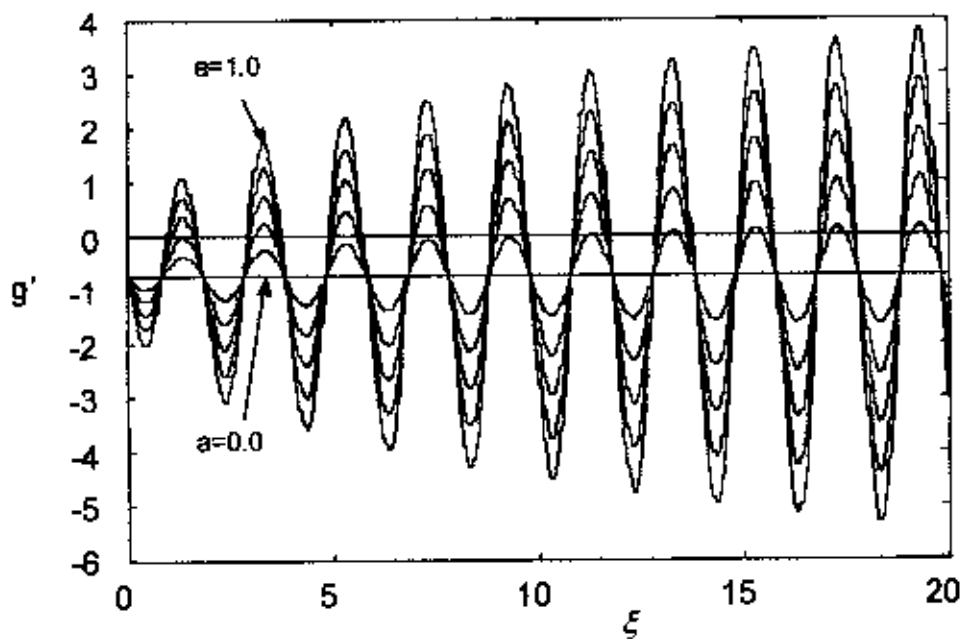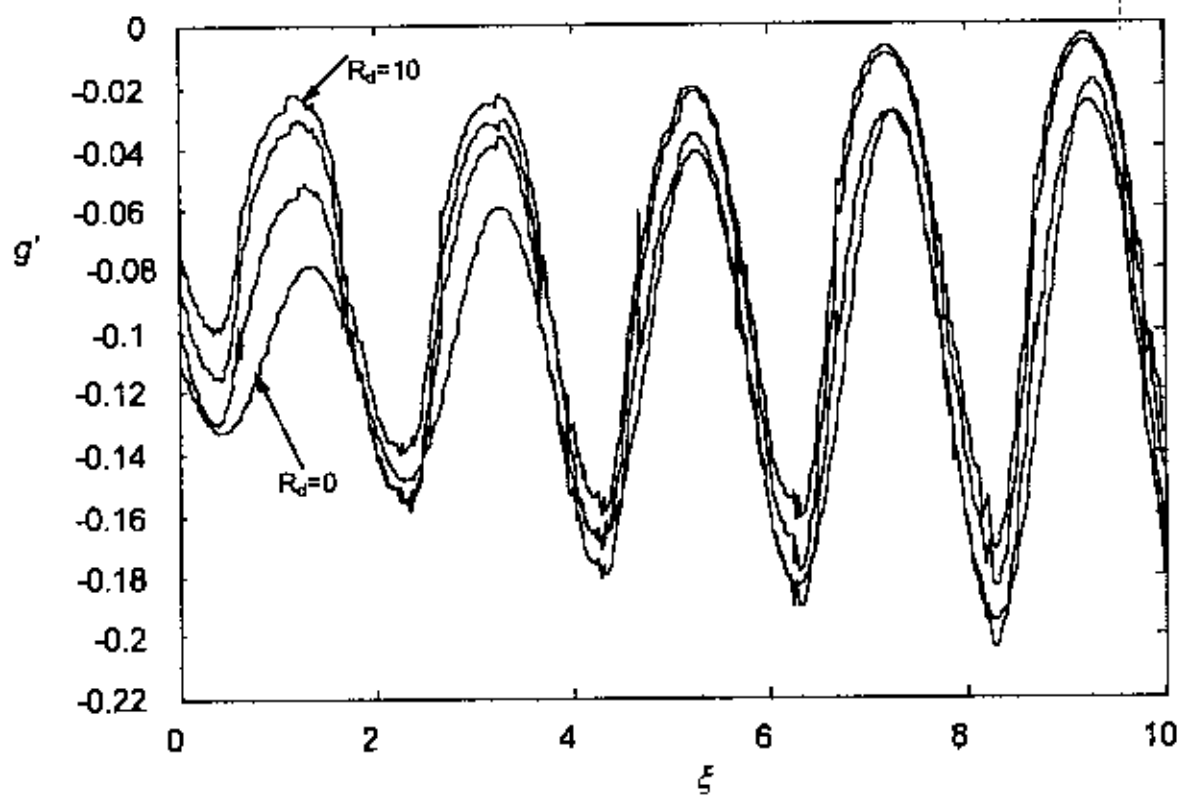

Fig 4.9: Rate of heat transfer against ξ for $R_d=0.0$, $a=0.0$, 0.2, 0.4, 0.6, 0.8, 1.0 at Pr.$=7.0$
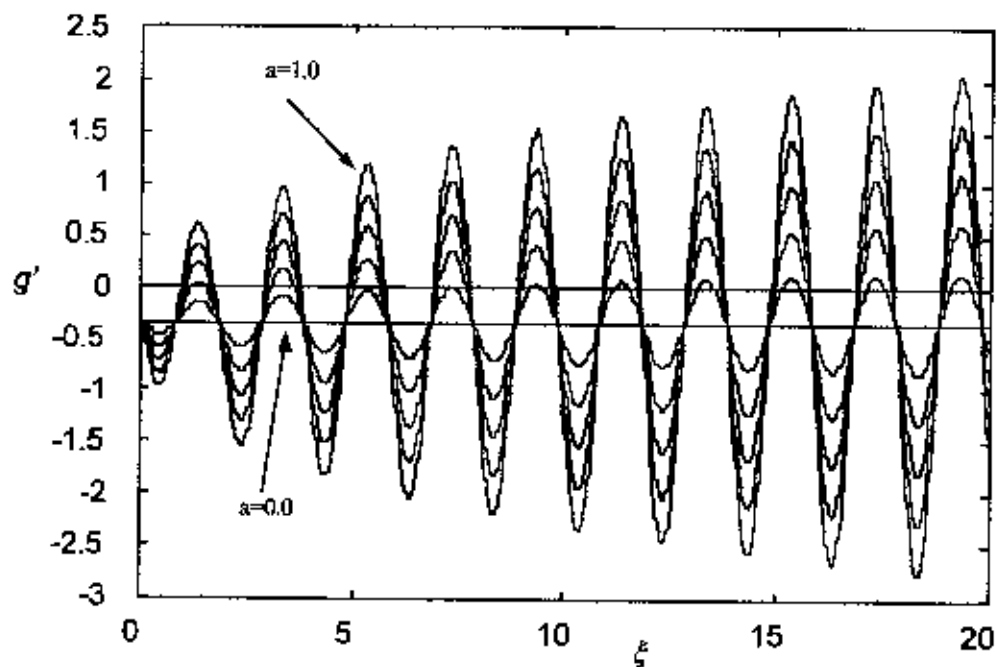
Fig 4.10: Rate of heat transfer against ξ for $R_d=0.0$, $a=0.0$, 0.2, 0.4, 0.6, 0.8, 1.0 at Pr.$=0.7$
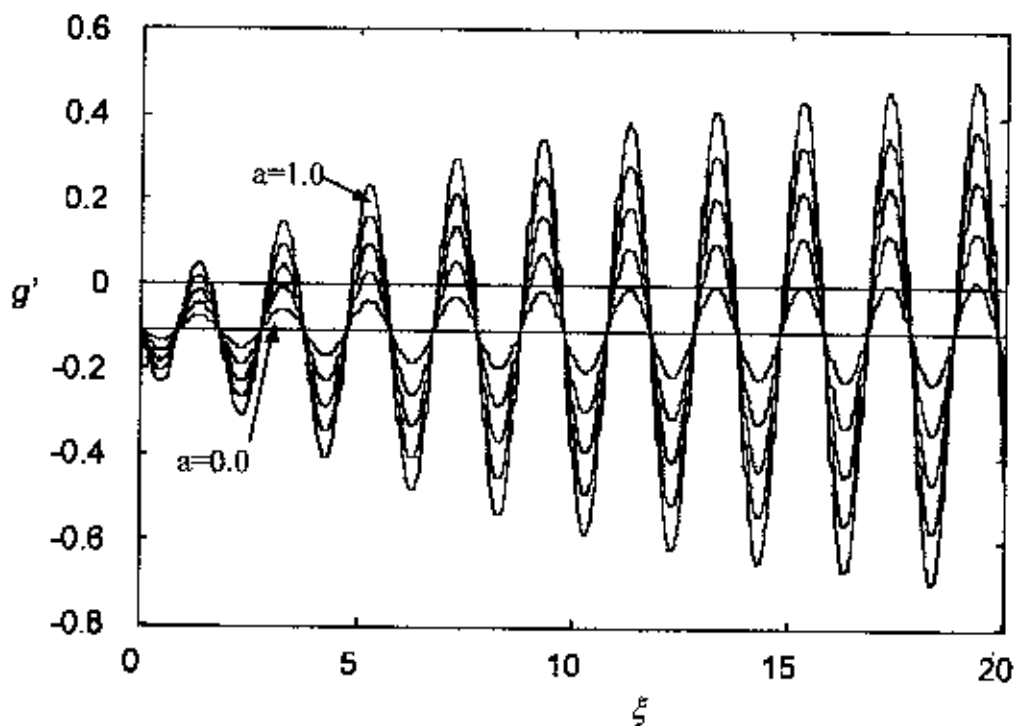
Fig 4.11: Rate of heat transfer against ξ for $R_d=0.0$, $a=0.0$, 0.2, 0.4, 0.6, 0.8, 1.0 at Pr.$=0.01$
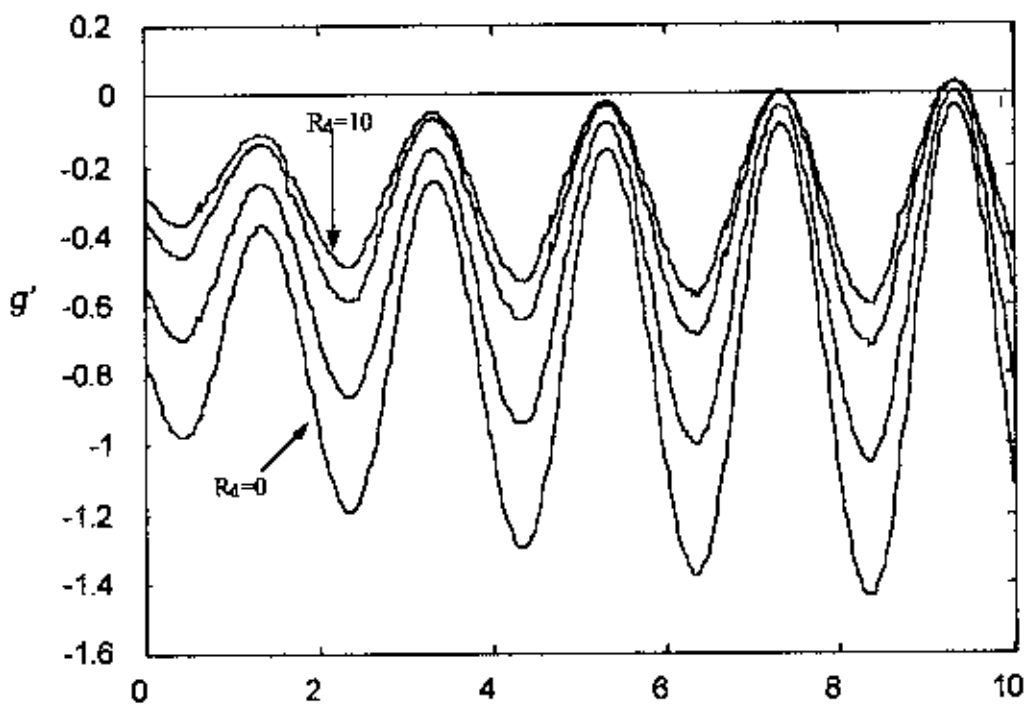
Fig 4.12: Rate of heat transfer against ξ for R_d=0.0, 1.0, 5.0, 10.0
a=0.2 at Pr.=7.0
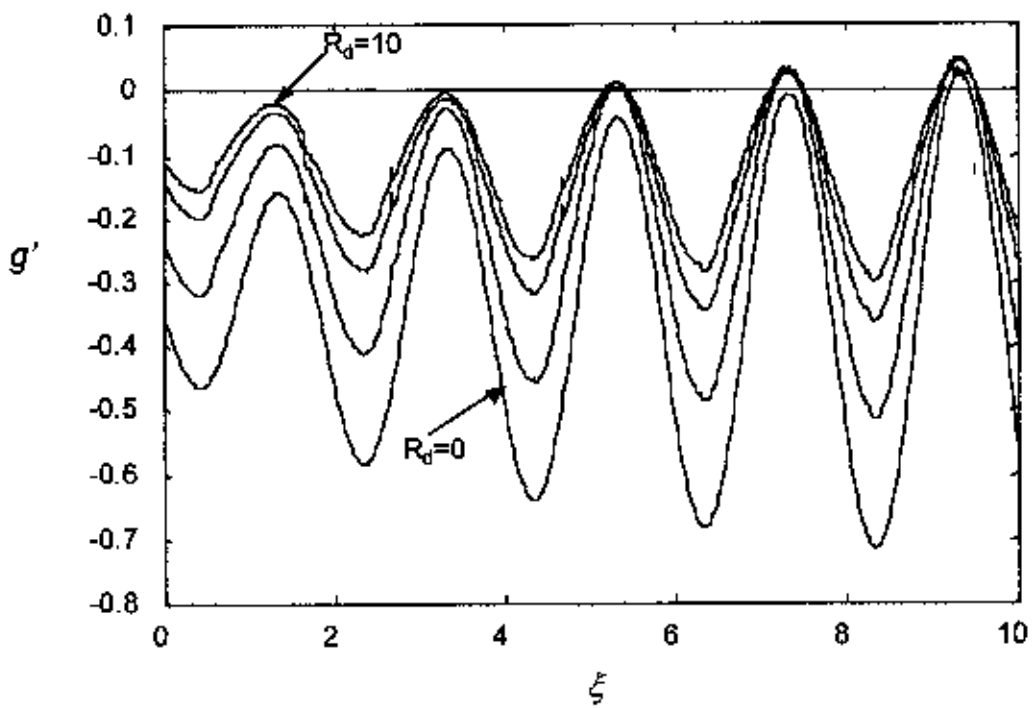
Fig 4.13: Rate of heat transfer against ξ for R_d=0.0, 1.0, 5.0, 10.0 a=0.2
at Pr.=0.7

Fig 4.14: Rate of heat transfer against ξ for R_d=0.0, 1.0, 5.0, 10.0 a=0.2 at Pr=0.01
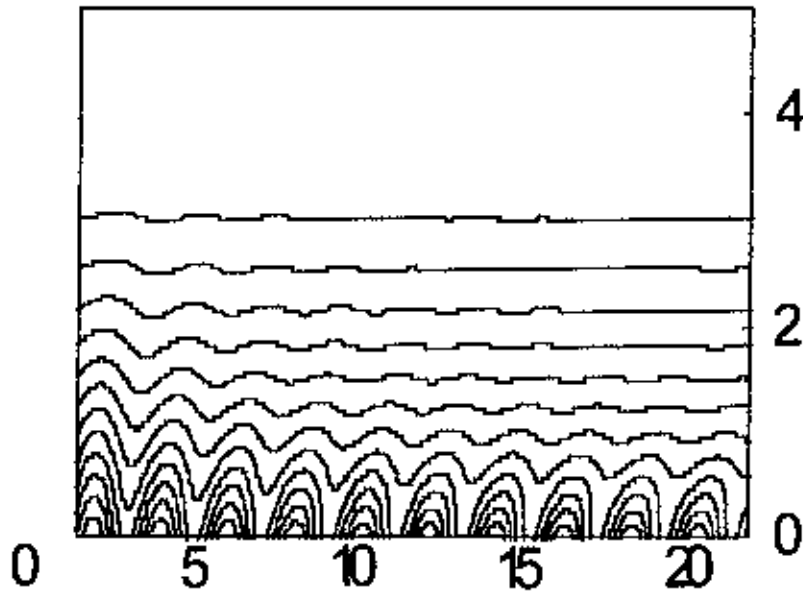
Fig: 4.15   Isotherms for Pr =0.7, a = 0.2, Rd =0.0
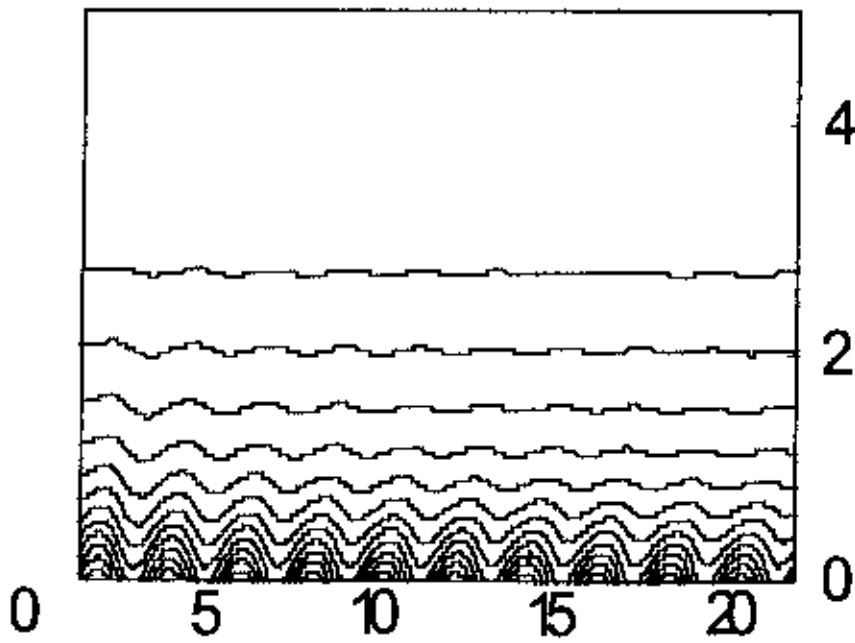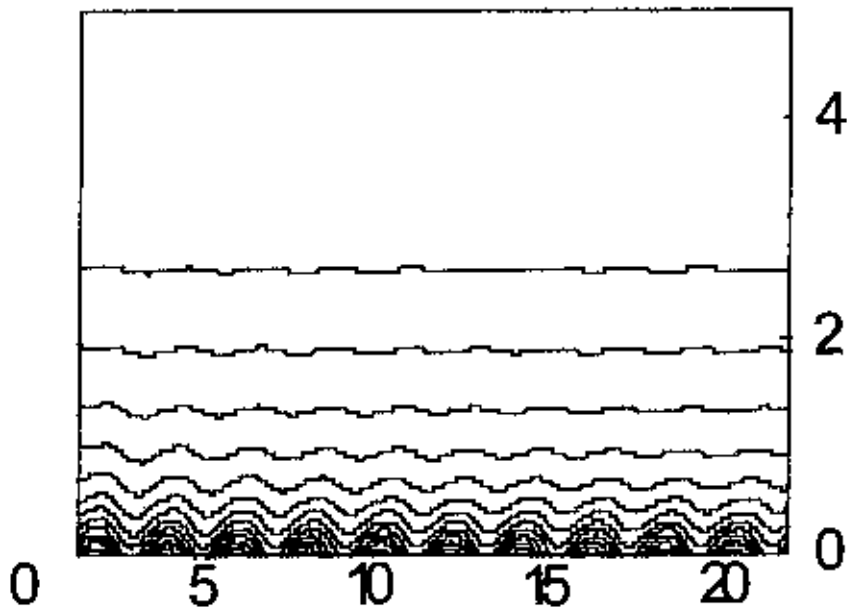

Fig: 4.16   Isotherms for Pr =0.7, a = 0.2, (b) Rd =5.0
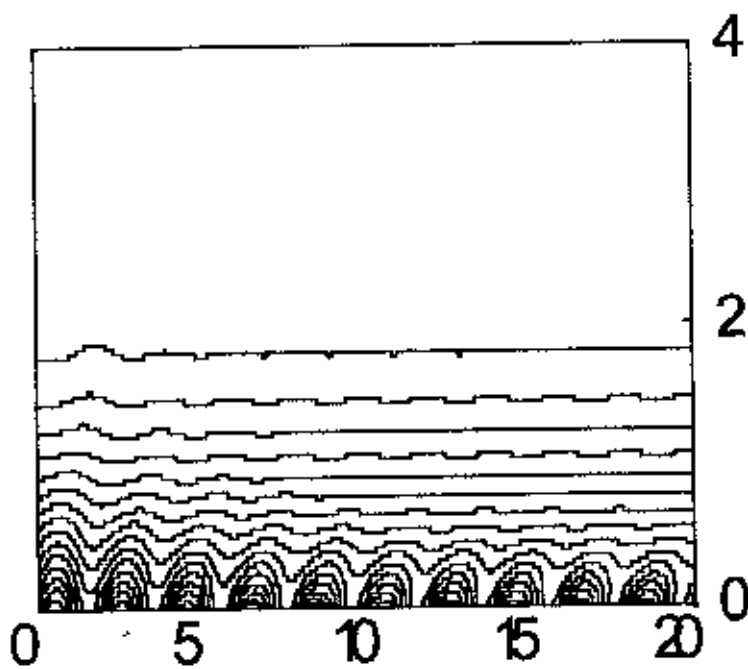
Fig: 4.17   Isotherms for Pr =0.7, a = 0.2, Rd =10.0

Fig 4.18 Isotherms for Pr =7.0, a = 0.2, Rd =0.0

40
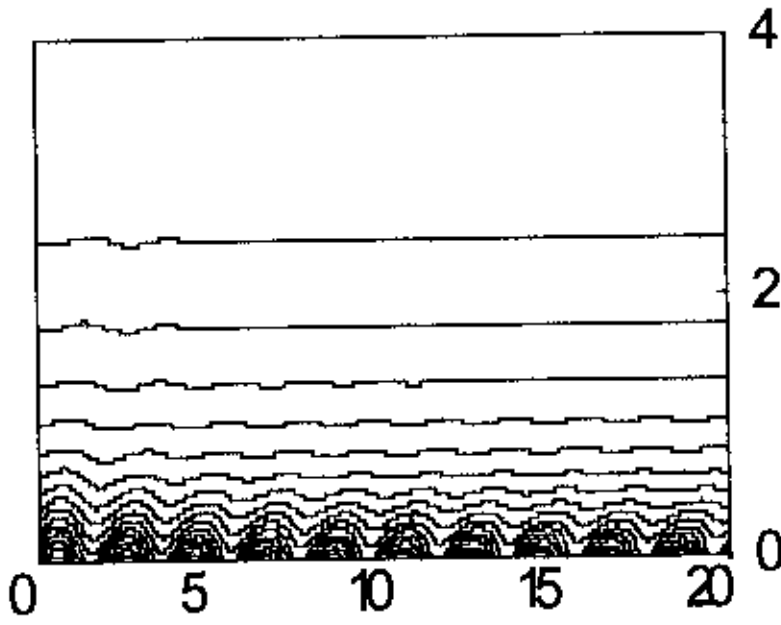
Fig 4.19 Isotherms for Pr =7.0, a = 0.2, Rd =5.0
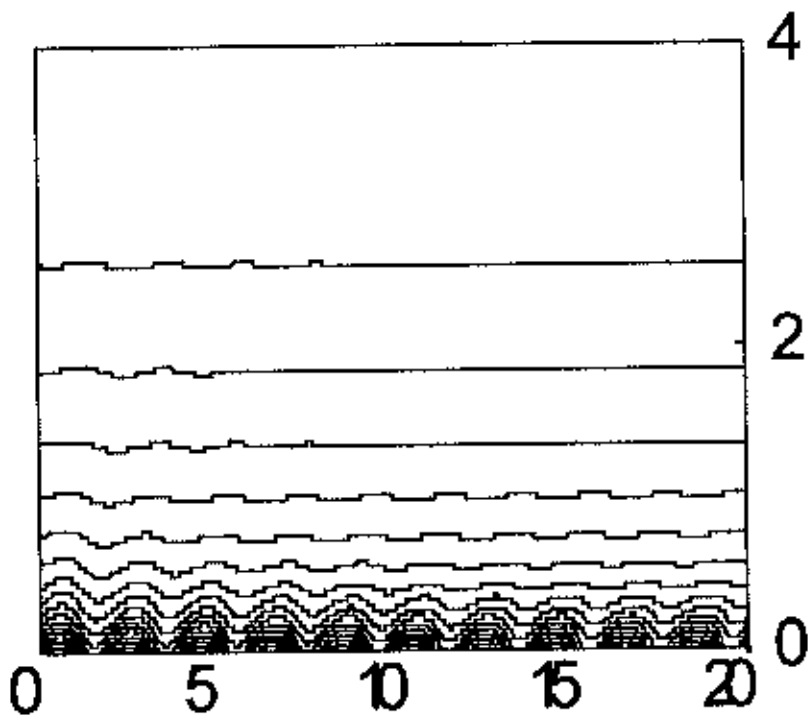

Fig 4.20 Isotherms for Pr =7.0, a = 0.2, Rd =10.0

41

Chapter 5

Effect of Radiation of steady streamwise surface temperature variations on a vertical Cone

Mathematical formalism

We consider a steady two-dimensional laminar free convection flow of the boundary layer induced by a heated semi-infinite surface immersed in an incompressible Newtonian fluid. In particular, the heated surface is maintained at the steady temperature, fluid having temperature, T, from a vertical cone. The physical coordinates (x, y) are chosen such that x is measured from the leading edge in the stream wise direction and y is measured normal to the surface of the cone. The coordinate system, velocity direction and the gravity orientation are shown in Figure 5.
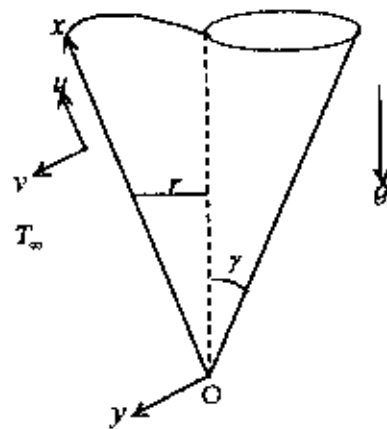

Figure 5: Physical model and co-ordinates

For this problem we have .

$$T = T_\infty + \left(T_w - T_\infty\right)\left(1 - a\sin(\pi\hat{x}d)\right)$$

(5.1)

42

where T_∞ is the ambient fluid temperature, T_w is the mean-surface temperature which is such that $T_w > T_\infty$, a is the relative amplitude of the surface temperature variations and 2d is the wavelength of the variations. The steady two-dimensional equations of motion are given by

$$\frac{\partial(r\,\hat{u})}{\partial \hat{x}} + \frac{\partial(r\,\hat{v})}{\partial \hat{y}} = 0 \tag{5.2}$$

$$\hat{u}\frac{\partial \hat{u}}{\partial \hat{x}} + \hat{v}\frac{\partial \hat{u}}{\partial \hat{y}} = -\frac{1}{\rho}\frac{\partial \hat{p}}{\partial \hat{x}} + \nu\nabla^2\hat{u} + g\beta(T-T_\infty)\cos\varphi \tag{5.3}$$

$$\hat{u}\frac{\partial T}{\partial \hat{x}} + \hat{v}\frac{\partial T}{\partial \hat{y}} = \frac{1}{Pr}\left[T_{yy} + \frac{16\sigma}{3\kappa(a+\sigma_s)}\left\{T^3 T_y\right\}_y\right] \tag{5.4}$$

with $\hat{r} = \hat{x}\sin\phi$

Boundary conditions are

$$\hat{u}=0,\quad \hat{v}=0,\quad T=T_\infty + (T_w-T_\infty)(1+a\sin\pi\tfrac{\hat{x}}{L})\ \text{at}\ \hat{y}=0 \tag{5.5}$$
$$\hat{u}=0,\quad T=T_\infty\ \text{as}\ \hat{y}\to\infty$$

Here Gr is the Grashof number and Pr is the Prandtl number. In the derivation of equations (5.2) the Boussinesq approximation has been assumed. We note that the

43

Grashof number has been based on d, half the dimensional wavelength of the thermal waves.

In the equations, u and v are, respectively, the velocity components in the x and y directions, T is the fluid temperature, v is the kinematic viscosity, β is the thermal expansion coefficient, α is the thermal diffusivity, κ is the thermal conductivity, a is the Rosseland mean absorption coefficient, σ is the Stephan-Boltzman constant, σ_s is the scattering coefficient

When the surface temperature is uniform and the Grashof number is very large, the resulting boundary-layer flow is self-similar. But the presence of sinusoidal surface temperature distributions, such as that given by (5.1), renders the boundary-layer flow non-similar. The boundary-layer equations are obtained by introducing the scaling

$$u = \frac{L}{v} Gr^{-\frac{1}{2}} \hat{u}, \quad v = \frac{L}{v} Gr^{-\frac{1}{4}} \hat{v}, \quad x = \frac{\hat{x}}{L},$$

$$y = \frac{\hat{y}}{L} Gr^{\frac{1}{4}}, \quad p = \frac{L^2}{\rho v^2} Gr^{-1} \hat{p}, \quad \theta = \frac{T - T_\infty}{T_w - T_\infty} \qquad (5.6)$$

into equations (5.2)-(5.4), formally letting Gr become asymptotically large and retaining only the leading order terms. Thus we obtain

$$u_x + v_y = 0 \qquad (5.7)$$

$$u u_x + v u_y = u_{yy} + \theta \qquad (5.8)$$

$$u \theta_x + v \theta_y = \frac{1}{\Pr}\left[\theta_{yy} + \frac{16\sigma}{3\kappa(a + \sigma_s)}\{\theta^3 \theta_y\}_y \right] \qquad (5.10)$$

Here the asterisk superscripts have been omitted for clarity of presentation. Equation (5.9) serves to define the pressure field in terms of the two velocity

· 44

components and is decoupled from the other three equations. Therefore, we shall not consider it further. As the equations are two-dimensional we define a stream function ψ, in the usual way.

$$u = \frac{1}{r}\psi_y, \quad v = -\frac{1}{r}\psi_x \tag{5.11}$$

and therefore, (5.7) is satisfied automatically. Guided by the familiar self-similar form corresponding to a uniform surface temperature, we use the substitution

$$\psi = x^{3/4} rf(\eta,x), \quad \theta = g(\eta,x), \quad r = x\sin\phi \tag{5.12}$$

where

$$\eta = y/x^{1/4} \tag{5.13}$$

is the pseudo-similarity variable. Equation (5.8) and (5.9) reduce to

$$f''' + g + \tfrac{7}{4} ff'' - \tfrac{1}{2} ff' + x(f_x f'' - f_x f') = 0 \tag{5.14}$$

$$\frac{1}{\text{Pr}}\left[\left\{1 + \frac{4}{3} R_d \left(1 + (\theta_w - 1)g\right)^3\right\}g'\right]' \tag{5.15}$$
$$+ \tfrac{7}{4} fg' + x(f_x g' - f g_x) = 0$$

and the boundary conditions are

$$f = 0, \quad f' = 0, \quad g = 1 + a\sin\pi x \tag{5.16}$$

at $\eta = 0$ and $f g \to 0$ as $\eta \to \infty$.

In equations (5.14)-(5.16), primes denote derivatives with respect to η.

45

3. Numerical solutions

The parabolic system of equations (5.14)-(5.16), is non-similar and its numerical solution must be obtained using a marching method. The results presented here were obtained using the Keller-box method, introduced by Keller and Cebeci [24] and described in more detail in Cebeci and Bradshaw [32]. After reduction of equations (5.14)-(5.15) to first-order form in η, the subsequent second-order accurate discretisation based halfway between the grid points in both the η- and x-directions (discussed detailed in Chapter 3) yields a set of nonlinear difference equations which are solved using a multi-dimensional Newton-Raphson iteration scheme. The results presented in Fig. 5.1 to Fig. 5.14 are based on uniform grids in both coordinate directions. There were 101 gridpoints lying between $\eta = 0$ and $\eta = 10$ and 201 between $x = 0$ and $x = 10$. We restrict the presentation of our results to the three values of the Prandtl number: Pr.=0.01(Liquid Metal) Pr. = 0.7 (air) and Pr. = 7 (water).

Fig. 5.1 shows the evolution with x of $f''(\eta = 0)$, a scaled surface shear stress, for constant values of the temperature wave amplitude, a, and the constant radiation parameter R_d for various values of Pr. In this figure we observed that as Pr. is decreasing skin friction is increasing. One point is mentionable that when Pr.=0.01, then wave amplitude is high than that of Pr.=7. As x increases, the amplitude of oscillation of the shear stress curves decays slowly.

We observe in Fig. 5.2- Fig.5.4 the evolution with x of surface shear stress, for various values of the temperature wave amplitude, a, and the constant radiation parameter R_d for different values of Pr. In these figure we observed that as Pr. is decreasing skin friction is increasing. We also observed as surface temperature wave amplitude is increasing shear stress is also increasing, and for decreasing of wave amplitude it is decreasing gradually.

Some aspects of the overall behaviour of these curves may be explained by observing that the boundary layer is thinner when the surface temperature is relatively high and thicker when it is low. This arises because relatively high surface temperatures induce relatively large upward fluid velocities with the consequent increase in the rate of entertainment into the boundary layer. This causes, in turn, a thinning of the boundary layer. Thus, we should expect high shear stresses and rates of heat transfer at, or perhaps just beyond, where the surface temperature attains its maximum values. There is an obvious qualitative difference between the curves shown in Fig. 5.1 and those in Fig. 5.4. As x increases, the amplitude of oscillation of the shear stress curves deceys slowly, with x.

Now we have to give our attention to the figure presented in Fig. 5.5 to Fig.5.7. Where the evolution with x of surface shear stress, for constant values of the temperature wave amplitude, a, and the various radiation parameter R_d for different values of Pr. The most interesting part of this analysis is that, when radiation parameter R_d is increasing skin friction is also increasing but when $R_d = 0$. the result of skin friction is exactly the same, which was found by Rees []. In our study we have found that skin friction is increasing as R_d is increasing but at a decreasing rate. That is, when $R_d = 1$ then skin friction is increased more in respect of $R_d = 10$.

Now we have to analyze the curves, which represents in Fig-5.8 to Fig-5.14, the local Nusselt number that is, the rate of heat transfer.

Fig. 5.8 shows the evolution with x of surface rate of heat transfer, for constant values of the temperature wave amplitude, a, and the constant radiation parameter R_d for various values of Pr. In this figure we observed that as Pr. is decreasing rate of heat transfer increasing. One point is mentionable that when Pr.$=7.0$, then wave amplitude is high than that of Pr.$=0.01$. As x increases, the amplitude of oscillation of the rate of heat transfer increasing significently.

Here we observe in Fig. 5.9 to Fig. 5.11 the evolution with x of surface rate of heat transfer, for various values of the temperature wave amplitude, a, and the constant radiation parameter R_d for different values of Pr. In these figures we observed that as Pr. is decreasing rate of heat transfer increasing. We also observed as surface temperature wave amplitude is increasing rate of heat transfer is also increasing, and for decreasing of wave amplitude it is decreasing gradually.

Important aspects of the overall behavior of these curves may be explained by observing that the boundary layer is thinner when the surface temperature is relatively high and thicker when it is low. This arises because relatively high surface temperatures induce relatively large upward fluid velocities with the consequent increase in the rate of entertainment into the boundary layer. This causes, in turn, a thinning of the boundary layer. Thus, we should expect high shear stresses and rates of heat transfer at, or perhaps just beyond, where the surface temperature attains its maximum values. There is an obvious qualitative difference between the curves shown in Fig. 5.8 to Fig. 5.11. As x increases, the amplitude of oscillation of the rate of heat transfer curves increases gradually, with x.

Indeed, the curves in Fig. 5.9 to Fig. 5.11 suggest that, whatever the value of a, there will always be a value of x beyond which some part of the rate of the heat transfer curve between successive surface temperature maxima will be positive. This somewhat unusual phenomenon for boundary layer flows may be explained by noting that when relatively hot fluid encounters a relatively cold part of the heated surface the overall heat transfer will be from the fluid into the surface, rather than the other way around.

Now we have to give our attention to the figures Fig. 5.12 to Fig.5.14 Where the evolution with x of surface rate of heat transfer, for constant values of the temperature wave amplitude, a, and the various radiation parameter R_d for different values of Pr. The most interesting part of this analysis is that, when radiation parameter R_d is increasing rate of heat transfer is also increasing but when $R_d = 0$. the result of rate of heat transfer is exactly the same, which was found by

Rees [14]. In our study we have found that rate of heat transfer is increasing as R_d is increasing but at a decreasing rate. That is, when $R_d = 1$ then rate of heat transfer increased more in respect of $R_d = 10$.
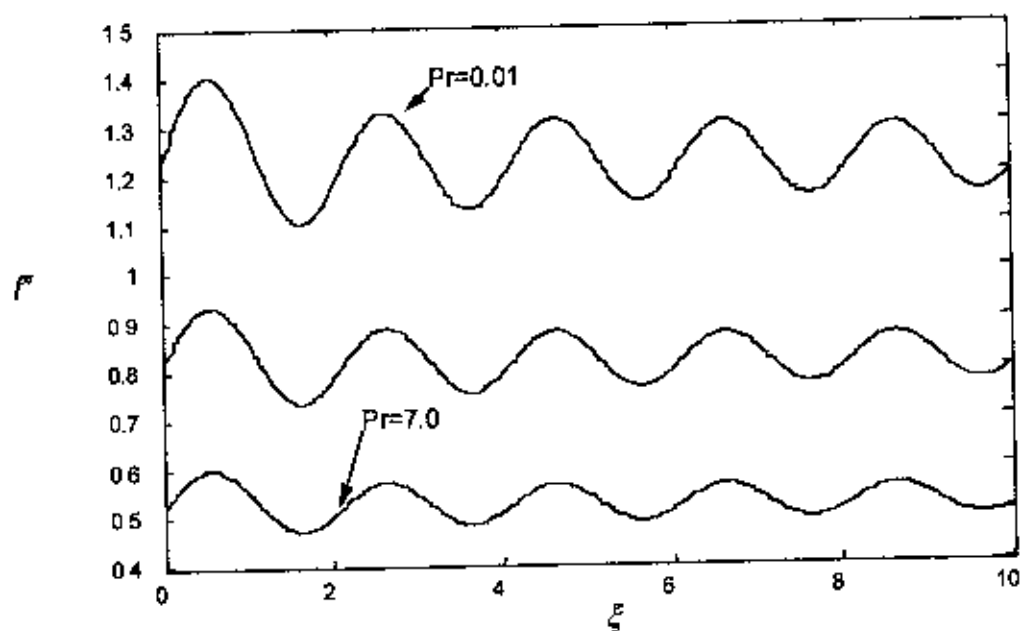
Presentation of Figure

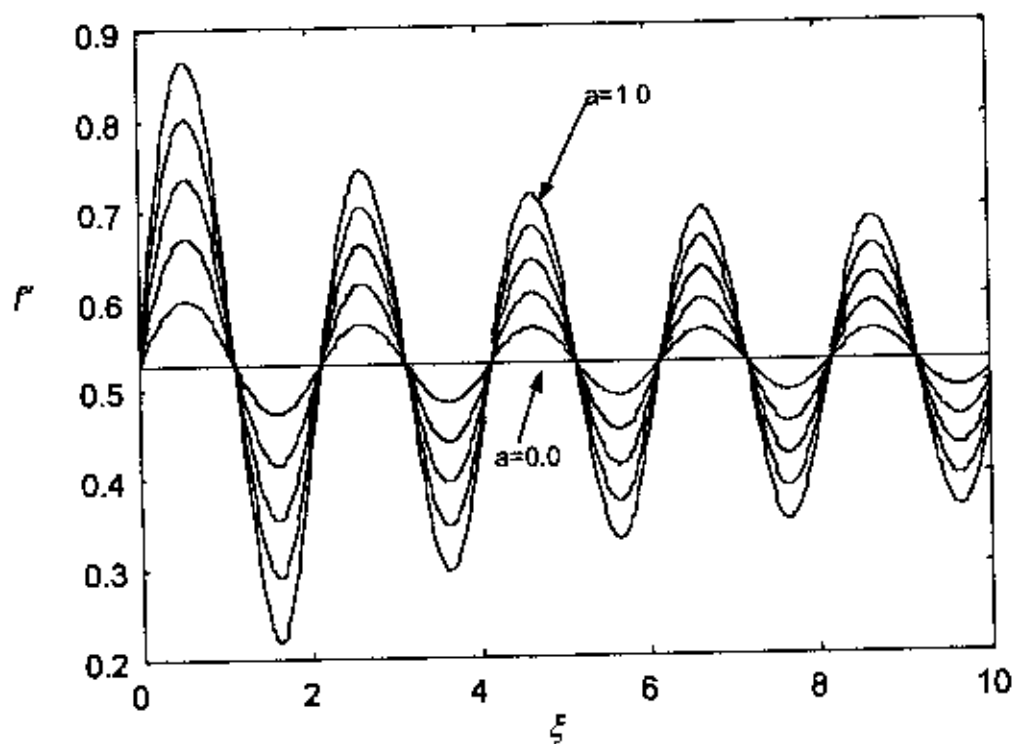Fig 5.1: Skin friction against ξ for $R_d=0.0$, $a=0.2$, Pr.=7.0, 0.7, 0.01.

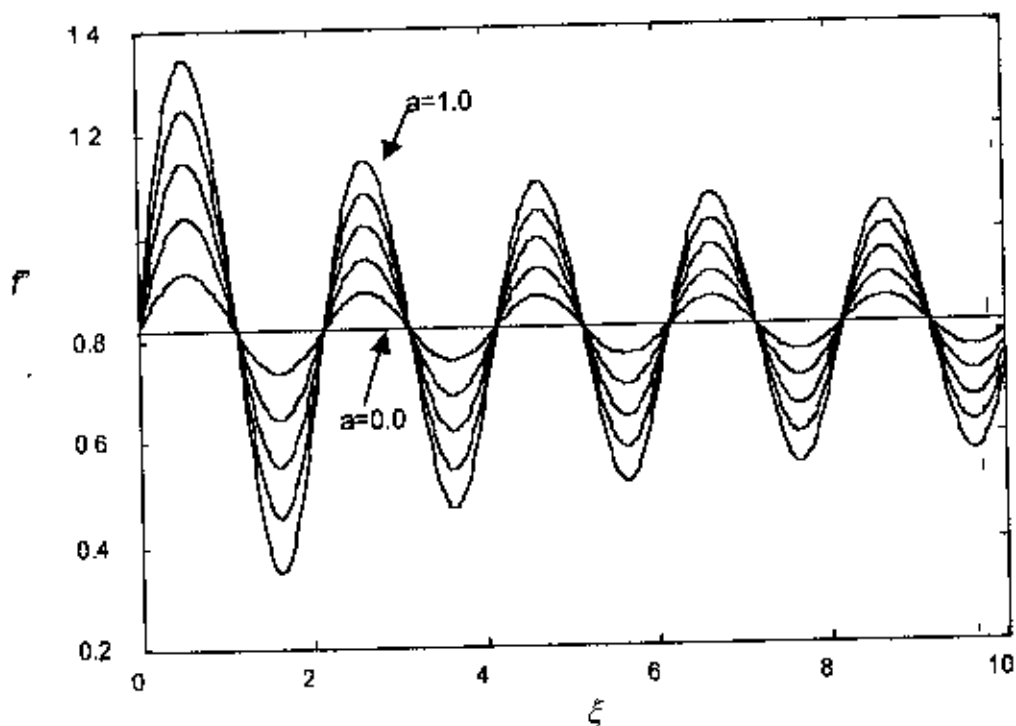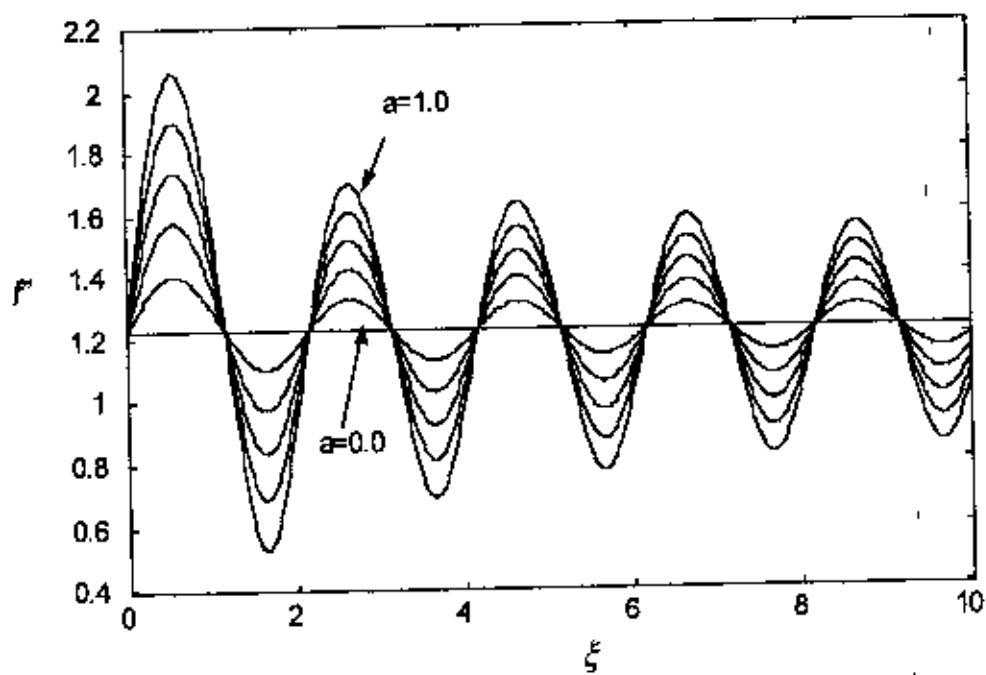Fig 5.2: Skin friction against ξ for $R_d=0.0$, $a=0.0$, 0.2, 0.4, 0.6, 0.8, 1.0 at Pr.=7.0

Fig 5.3: Skin friction against ξ for R_d=0.0, a=0.0, 0.2, 0.4, 0.6, 0.8, 1.0 at Pr.=0.7

Fig 5.4: Skin friction against ξ for R_d=0.0, a=0.0, 0.2, 0.4, 0.6, 0.8, 1.0 at Pr.=0.01
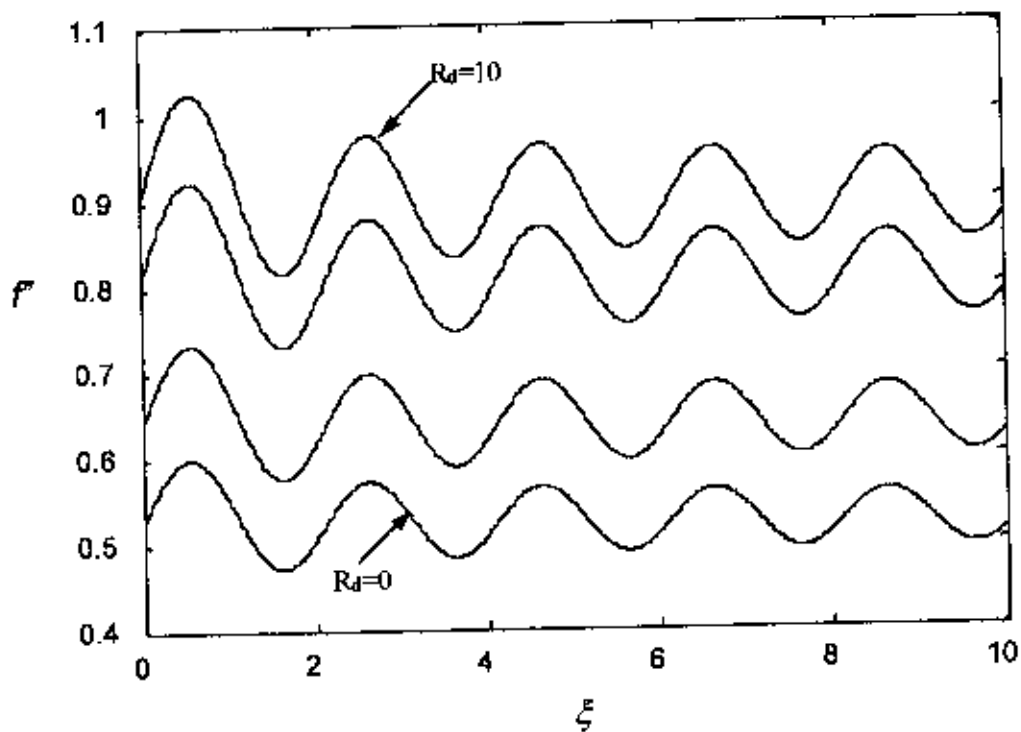
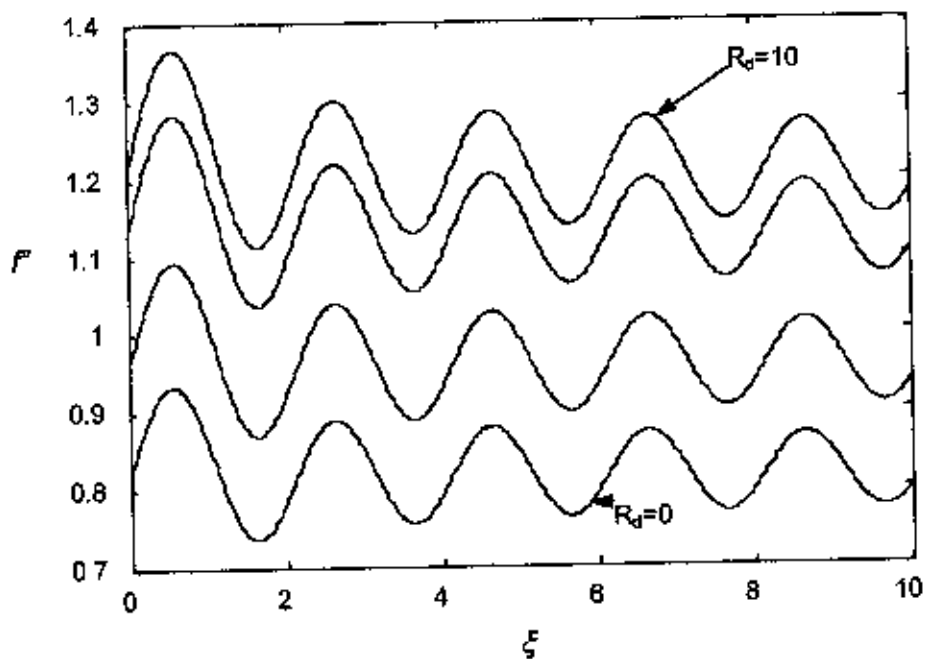Fig 5.5: Skin friction against ξ for R_d=0.0, 1.0, 5.0, 10.0 a=0.2, at Pr.=7

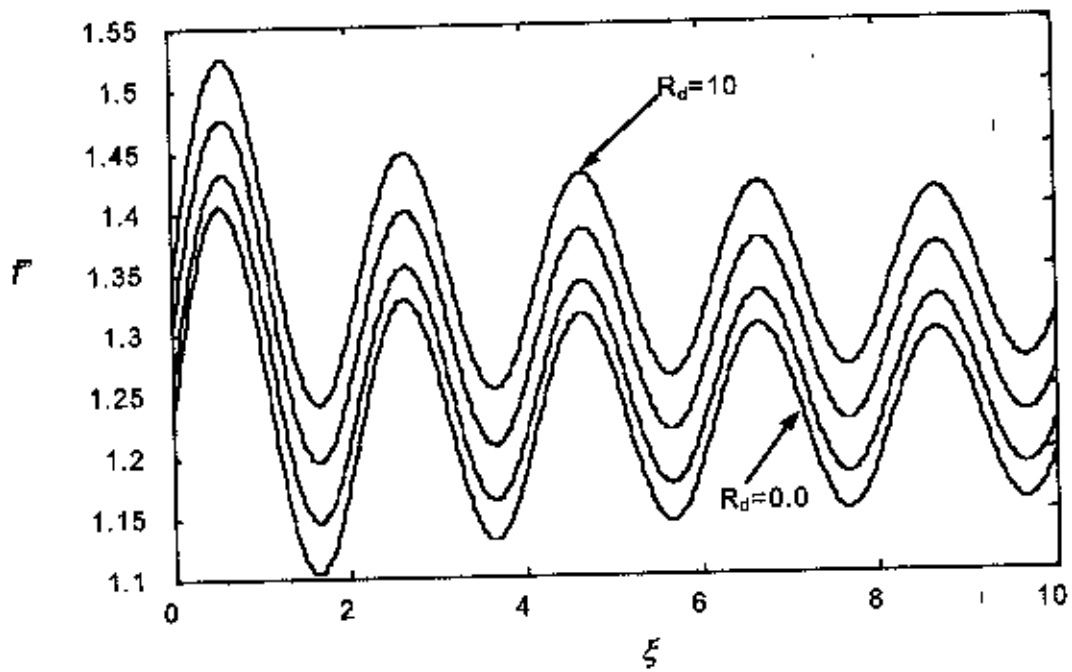Fig 5.6: Skin friction against ξ for R_d=0.0, 1.0, 5.0, 10.0 a=0.2, at Pr.=0.7

53

Fig 5.7: Skin friction against ξ for R_d=0.0, 1.0, 5.0, 10.0 a=0.2, at
Pr.=0.01
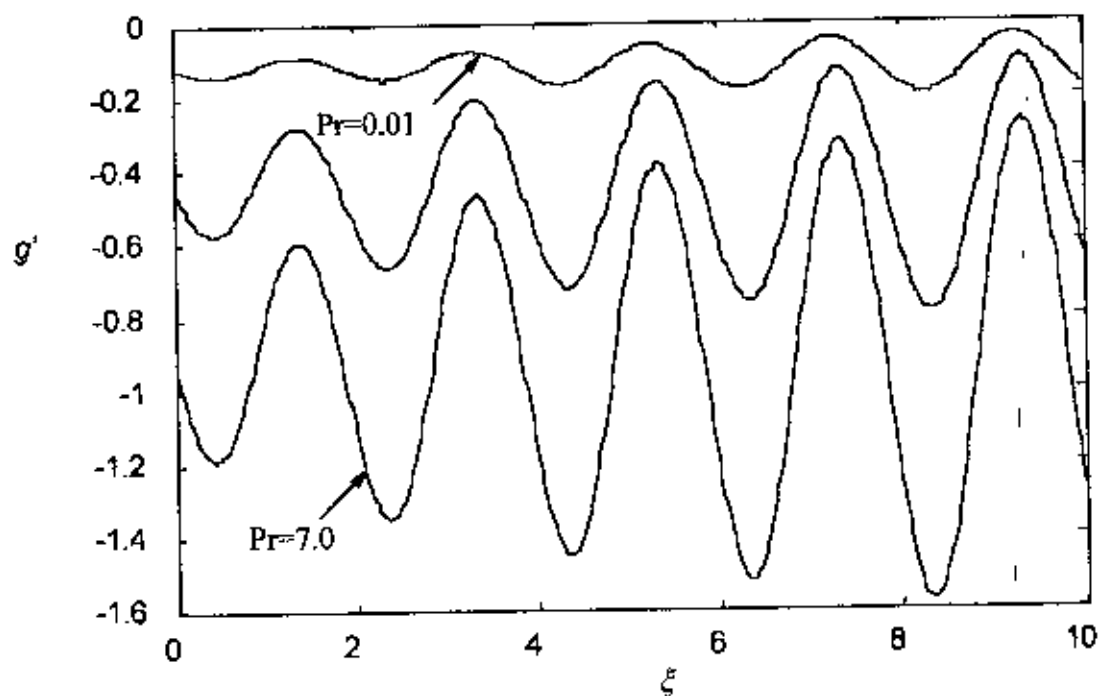
Fig 5.8: Rate of heat transfer against ξ for $R_d=0.0$, a=0.2, Pr.=7.0, 0.7, 0.01.

Fig 5.9: Rate of heat transfer against ξ for $R_d=0.0$, a=0.0, 0.2, 0.4, 0.6, 0.8, 1.0 at Pr.=7.0

Fig 5.10: Rate of heat transfer against ξ for $R_d=0.0$, a=0.0, 0.2, 0.4, 0.6, 0.8, 1.0 at Pr.=0.7
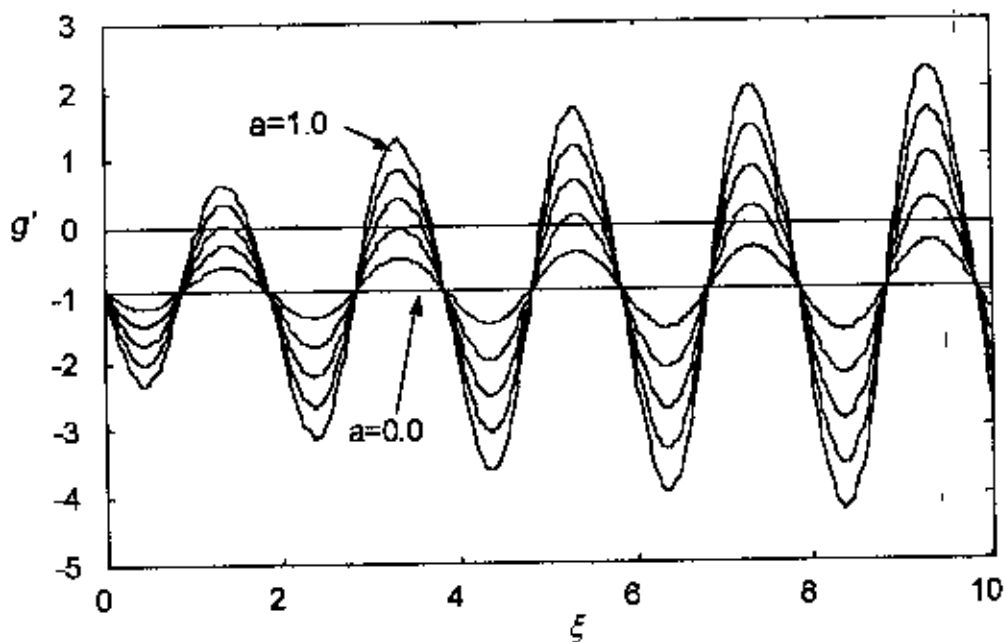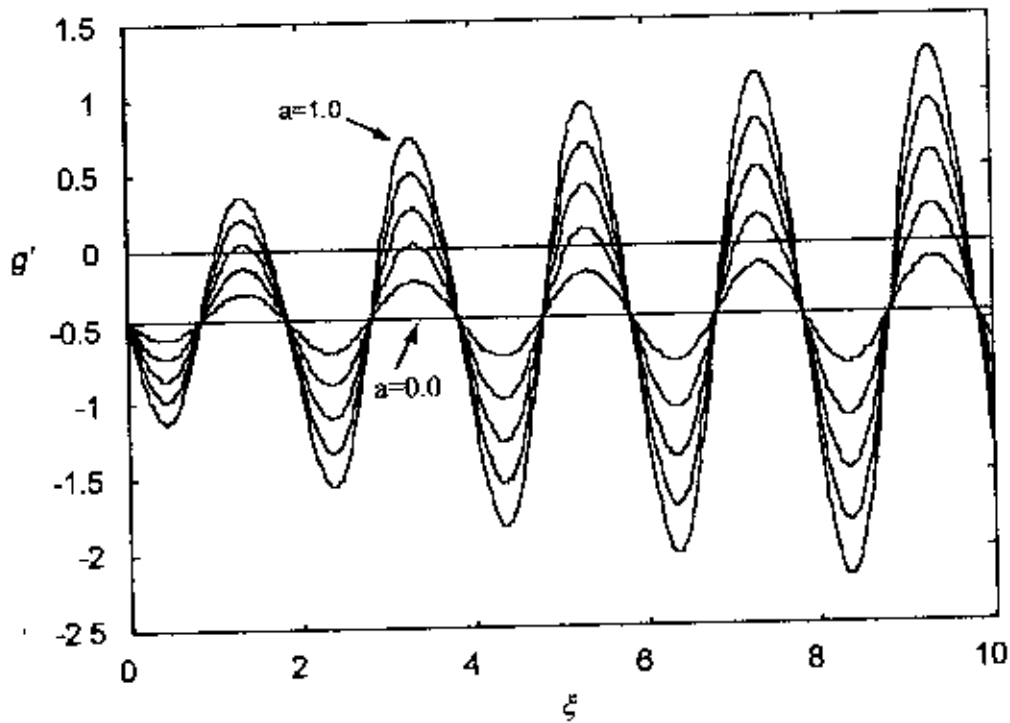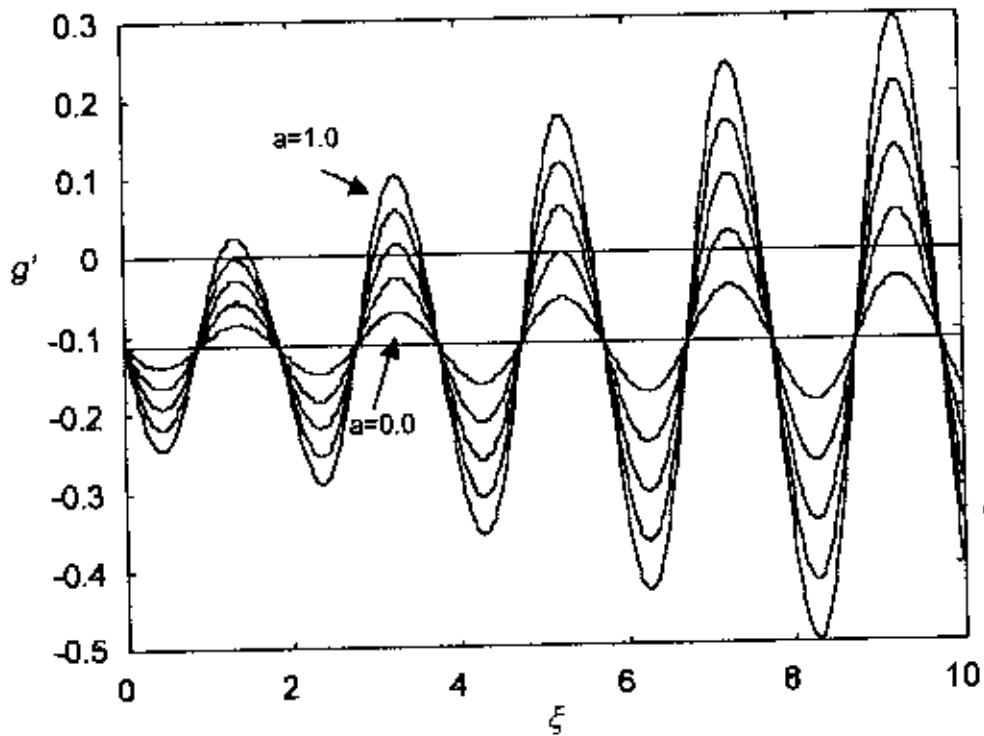

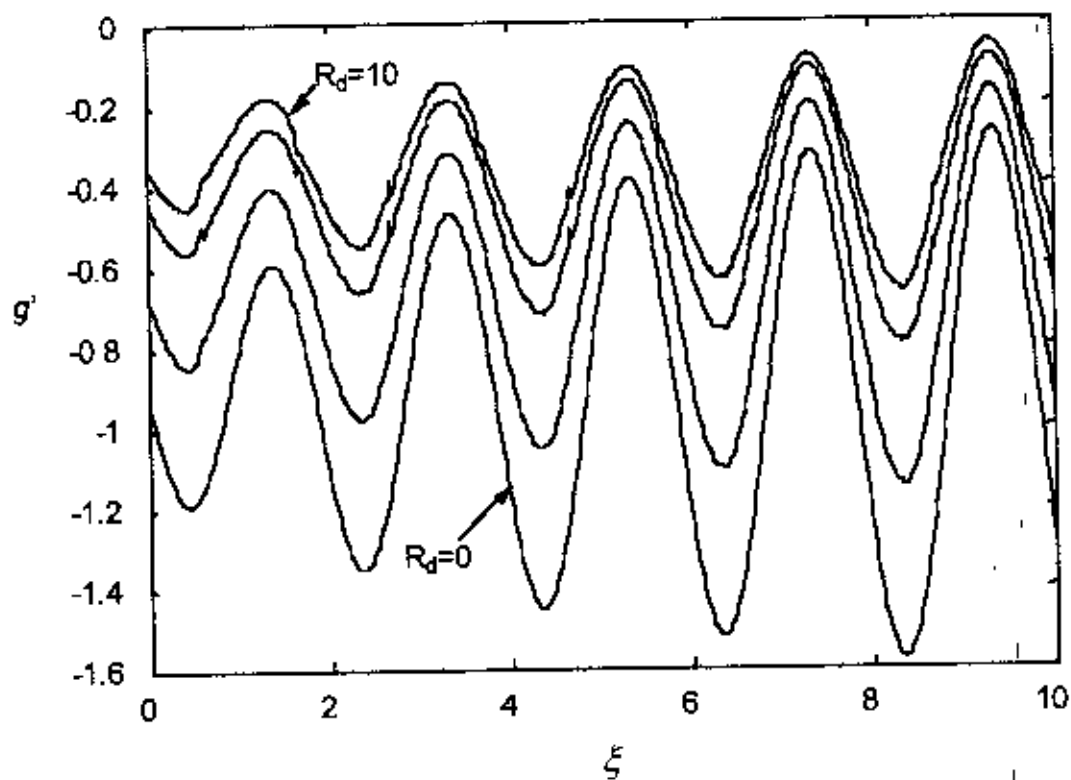Fig 5.11: Rate of heat transfer against ξ for $R_d=0.0$, a=0.0, 0.2, 0.4, 0.6, 0.8, 1.0 at Pr.=0.01

Fig 5.12: Rate of heat transfer against ξ for R_d=0.0, 1.0, 5.0, 10.0 a=0.2 at Pr.=7.0
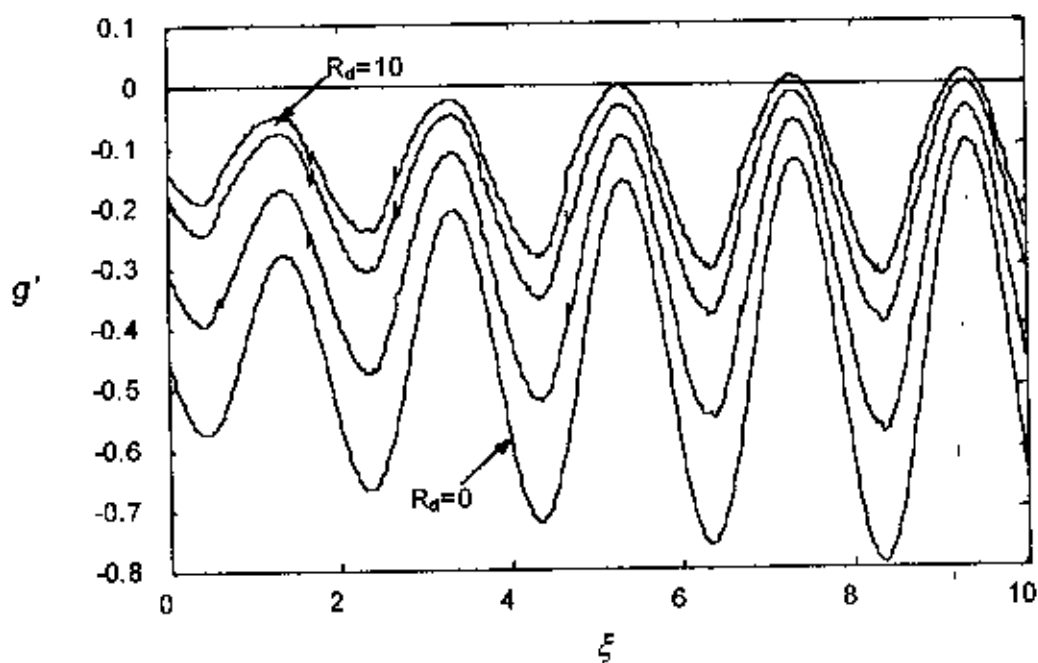

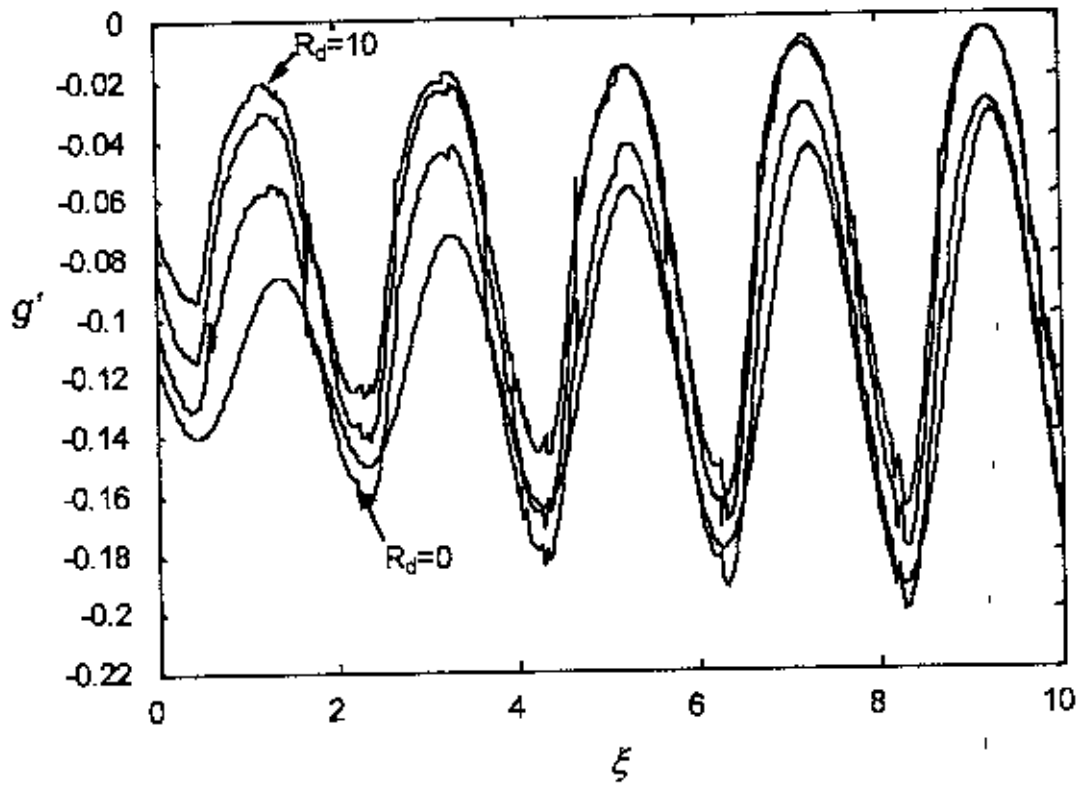Fig 5.13: Rate of heat transfer against ξ for R_d=0.0, 1.0, 5.0, 10.0 a=0.2 at Pr.=0.7

57

Fig 5.14: Rate of heat transfer against ξ for R_d=0.0, 1.0, 5.0, 10.0
a=0.2 at Pr.=0.01

Chapter 6

Conclusions

We have analyzed the effect of radiation-conduction interaction with steady streamwise surface temperature variations on vertical free convection as well as vertical cone has been investigated numerically using a finite difference method. The effect of variations in the Plank number, the surface temperature wave amplitude, and the Prandtl number on the shear stress and rate of surface heat transfer have been presented graphically.

We have restricted the presentation of our results to the three values of the Prandtl number: Pr.=0.01(Liquid Metal) Pr. = 0.7 (air) and Pr. = 7 (water).

In our study we observed that as Pr. is decreasing skin friction is increasing. One point is mentionable that when Pr.=0.01, then wave amplitude is high than that of Pr.=7. As x increases, the amplitude of oscillation of the shear stress curves decays slowly.

Physical aspects of the overall behaviour of these result may be explained by observing that the boundary layer is thinner when the surface temperature is relatively high and thicker when it is low. This arises because relatively high surface temperatures induce relatively large upward fluid velocities with the consequent increase in the rate of entertainment into the boundary layer. This causes, in turn, a thinning of the boundary layer. Thus, we should expect high shear stresses and rates of heat transfer at, or perhaps just beyond, where the surface temperature attains its maximum values.

The most interesting part of this analysis is that, when radiation parameter R_d is increasing skin friction is also increasing but when R_d =0. the result of skin friction is exactly the same, which was found by Rees [14]. In our study we have found that skin friction is increasing as R_d is increasing but at a decreasing

rate. That is, when $R_d = 1$ then skin friction is increased more in respect of $R_d = 10$.

Now we have to analyze the local Nusselt number that is, the rate of heat transfer.
We observed that as Pr. is decreasing rate of heat transfer increasing. One point is mentionable that when Pr.=7.0, then wave amplitude is high than that of Pr.=0.01. As x increases, the amplitude of oscillation of the rate of heat transfer increasing significantly.

The surface rate of heat transfer, for various values of the temperature wave amplitude, a, and the constant radiation parameter R_d for different values of Pr. In this case we observed that as Pr. is decreasing, rate of heat transfer increasing. We also observed as surface temperature wave amplitude is increasing rate of heat transfer is also increasing, and for decreasing of weve amplitude it is decreasing gradually.

Important aspects of the overall behavior of these curves may be explained by observing that the boundary layer is thinner when the surface temperature is relatively high and thicker when it is low. This arises because relatively high surface temperatures induce relatively large upward fluid velocities with the consequent increase in the rate of entertainment into the boundary layer. This causes, in turn, a thinning of the boundary layer. Thus, we should expect high shear stresses and rates of heat transfer at, or perhaps just beyond, where the surface temperature attains its maximum values.

Now we have to give our attention to the surface rate of heat transfer, for constant values of the temperature wave amplitude, e, and the various radiation parameter R_d for different values of Pr. The most interesting part of this analysis is that, when radiation parameter R_d is increasing rate of heat transfer is also increasing but when $R_d = 0$. the result of rate of heat transfer is exactly the same, which was found by Rees [14]. In our study we have found that rate of heat transfer is increasing as R_d is increasing but at a decreasing rate. That is, when $R_d = 1$ then rate of heat transfer increased more in respect of $R_d = 10$.

References

1. Arpaci, V. S.: Effect of thermal radiation with free convection from a heated vertical plate, *Int. J. Heat Mass Transfer*, 15, 1243-1252 (1972).
2. Bankston, J. D., Lloyd, J. R. and Novonty, J. L.: Radiation convection interaction in an absorbing-emitting liquid in natural convection boundary layer flow, *J. Heat Transfer*, 99, 125-127 (1977).
3. C. P. Chiu, H.M. Chou, Free convection in the boundary layer flow of a micropolar fluid along a vertical wavy surface. Acta Mechanica 101 (1993) 161-174.
4. Cess, R. D.: Interaction of thermal radiation with free convection heat transfer, *Int. J. Heat Mass Transfer*, 9, 1269-1277 (1966).
5. Cheng, E. H. and Ozisik, M. N.: Radiation with free convection in an absorbing, emitting and scattering medium, *Int. J. Heat Mass Transfer*, 15, 1243-1252 (1972).
6. Cogley, A. C., Vincenti, W. G. and Giles, S. E.: Differential approximation for radiative in a non-gray gas near equilibrium, *AIAA J.*, 6, 551-553 (1968).
7. Chandrasekhar, S., *Radiative Heat Transfer*, Dover, New York, (1960).
8. D. A. S. Rees, I. Pop. A note on free convection along a vertical wavy surface in a porous medium. Trans. ASME ASME Journal of Heat Transfer 116 (1994) 505-508.
9. D. A. S. Rees. I Pop, Free convection induced by a horizontal wavy surface in a porous medium. Fluid Dynamics Research 14 (1994) 151-166.
10. D. A. S. Rees, I. Pop, Free convection induced by a vertical wavy surface with uniform heat flux in a porous medium. Trans. ASME Journal of Heat Transfer 117 (1995) 547-550.
11. D. A. S. Rees, I. Pop, Non-Darcy natural convection from a vertical wavy surface in a porous medium. Transport in porous Media 20 (1995), 223-234.
12. D. A. S. Rees, I. Pop, The effect of longitudinal surface waves on free convection from vertical surfaces in porous media. Int. Comm. Heat Mass Transfer 24 (1997) 419-425.

13. D. A. S. Rees Three dimensional free convection boundary layers in porous media induced by a heated surface with spanwise temperature variation. Trans. ASME Journal of Heat Transfer 119 (1997) 792-798.

14. D. A. S. Rees The effect of steady streamwise surface temperature variation on vertical free convection Int. Journal of Heat Mass Transfer 42 (1999) 2455-2464.

15. E. Kim. Natural convection along a wavy vertical plate to non-Newtonian fluids. International Journal of Heat Mass Transfer 40 (1997) 3069-3078.

16. E. M. Sparrow, J. L. Gregg. Similar solution for free convection from a non isothermal vertical plate. Trans. ASME Journal of Heat Transfer 80 (1958), 379-384.

17. Greif, R. Habib, I. S. and Lin, J. C. , Laminar free convection of a radiating gas in vertical channel, J. *Fluid Mechanics*, 46, 513-520 (1971).

18. Hasegawa, S. Echigo, R. and Fakuda, K.: Analytic and experimental studies on simultaneous radiative and free convective heat transfer along a vertical plate, *Proc. Japanese Soci. Mech. Engineers*, 38, 2873 - 2883 and 39, 250-257 (1972.)

19. Hossain, M. A. and Takhar, H. S.: Radiation effect on mixed convection along a vertical plate with uniform surface temperature, *Heat Mass Transfer*, 35, 243-248 (1996).

20. Hossain, M. A. and Alim, M. A.: Natural convection-radiation interaction boundary layer flow along a thin vertical cylinder , *Heat and Mass Transfer*, 36, 515-520 (1997).

21. Hossain, M. A., Alim, M. A. and S. Takhar, H. S.: Mixed convection boundary layer flow along a vertical cylinder, *J. Appld. Mech. Engng.* (1998), (In press).

22. Hossain, M. A., K. C. A. Alam I. Pop. MHD free convection flow along a vertical wavy surface with uniform surface temperature submitted for publication.

23. Hossain, M. A. and Rees, D. A. S., Radiation-conduction interaction on mixed convection flow along a slender vertical cylinder, AIAA J. Thermophysics and Heat Transfer, 12, (1998) 611-614.

24. H. B. Keller, T. Cebeci. Accurate numerical methods for boundary layer flows. Two dimensional flows. Proc. Int. Cont. Numerical Methods in Fluid Dynamics. Lecture Notes in Physics. Springer New York. 1971.

25. L. L. Yao, Natural convection along a vertical wavy surface. Trans. ASME Journal of Heat Transfer 105 (1983), 465-468.

26. S. Ostrach, An analysis of laminar free convection flow and heat transfer about a flat plate parallel to the direction of the generating body force. NACA IV 2635, 1952.

27. M. Kutubuddin, M. A. Hossain and H. S Thakar, Radiation interaction on forced and free convection across a horizontal cylinder, Applied Mechanics and Engineering vol. 4, No.2, pp.219-235, 1999

28. Soundalgekar V. M. and Takhar H. S.: Radiative free convection flow of gas past a semi-infinite vertical plate, *Modeling, Measurement and Control*, B51, 31-40 (1993).

29. Sparrow, E. M. and Cess, R. D.: *Radiation Heat Transfer, Int. J. Heat Mass Transfer*, 5, 179-806 (1962).

30. S. G. Moulic. L. S. Yao. Mixed convection along a wavy surface. Trans. ASME Journal of Heat Transfer 111, (1989), 974-979.

31. S. G. Moulic, L. S. Yao. Natural convection along a vertical wavy surface with uniform heat flux. Trans. ASME Journal of Heat Transfer 111(1989), 1106-1108.

32. T. Cebeci, P. Bradshaw, Physical and Computational Aspects of Convection Heat Transfer. Springer, New York. 1984.

33. M. Kutubuddin, M. A. Hossain and I. Pop, Effect of conduction-radiation interaction on the mixed convection flow from a horizontal cylinder, Heat and Mass Transfer 35(1999) 307-314

34. Merk, E. J. and Prins, J. A.: Thermal convection in laminar boundary layer I. *Appl. Sci. Res.*, vol-4A, pp. 11-24 (1953).

35. Merk, E. J. and Prins, J. A.: Thermal convection in laminar boundary layer II. *Appl. Sci. Res.*, vol-4A, pp. 195-206 (1954).

36. Broun, W. H., Ostrach, S. and Heighway, J. E.: Free convection similarity flows about two-dimensional and axisymmetric bodies with closed lower ends. *Int. J. Heat Mass Transfer*, vol. 2, pp. 121-135.(1961)

37. Hering, R. G. and Grosh, R. J.: Laminar free convection from a non-isothermal cone. *Int. Haat Mass Transfer,* vol-5, pp. 1059-1068 (1962).

38. Hering, R. G.: Laminar free convection from a non-isothermal cone at low Prandtl numbers. *Int. J. Heat Mass Transfer* vol-8, pp. 1333-1337 (1965).

39. Roy, S.: Free convection over a slender vertical cone at high Prandtl numbers. *ASME J. Haat Transfer* vol-101, pp.174-176 (1974).

40. Na, T. Y. and Chiou, J. P.: Laminar natural convection over a frustum of a cone. *Appl. Sc. Res.* vol-35, pp. 409-421 (1979).

41. Sparrow, E. M. and Guinle, L. D. F.: Deviation from classical free convection boundary layer theory at low Prandtl numbers. *Int. J. Heat Mass Transfer* vol-11, pp. 1403-1415 (1968).

42. Lin, F. N.: Laminar free convection from a vertical cone with uniform surface heat flux. *Letters in Heat and Mass Transfer,* vol-3, pp. 45-58 (1976).

43. Kuiken, H. K.: Axisystemmetric free convection boundary layer flow past slender bodies. *Int. J. Heat Mass Transfer,* vol-11, pp. 1141-1153 (1968).

44. Oosthuizen, P. H. and Donaldson, E.: Free convection heat transfer from vertical cones. *J. Heat Transfer.,* Trans ASME 94 C3 pp. 330-331 (1972).

45. Na, T. Y. and Chiou J. P.: Laminar natural convection over a slender vertical frustum of a cone. *Warme und Stoffubertraegung,* vol-12, pp. 83-87 (1979).

46. Na, T. Y. and Chiou, J. P.: Laminar natural convection over a slender vertical frustum of a cone with constant wall heat flux. *Warme und Stoffubertraagung* vol-12, pp. 83-87 (1980).

47. Alamgir, M.: Over-all heat transfer from vertical cones in laminar free convection: an approximate method. *ASME J. Heat Transfer* vol-101, pp. 174-176 (1989).

48. M. A. Hossain and S. C. Paul, Free convection from a vertical permeable circular cone with non-uniform surface temperature, Applied Scientific Research (1999) (submitted).

49. Butcher, J. C.: Implicit Runge-Kutta process. *Math. Comp.,* vol-18, pp.50-55 (1974).

50. Nachtsheim, P. R. and Swigert, P.: Satisfaction of Asymptotic Boundary Conditions in Numerical Solutions of Systems of Non-linear Equations of Boundary-layer Type, NASA TN-D3004 (1965).

51. Siegel, R. and Howell, J. R.: *Thermal Radiation Heat Transfer*, McGraw-Hill, N. Y. (1987)

52. T. S. Chen: Parabolic systems: local non-similarity method, *Handbook of Numerical Heat Transfer*, (ed by W. J. Minkowycz, et al. Chap. 5), Wiley, New York (1988).